BELLCOMM, INC.
955 L'ENFANT PLAZA NORTH, S.W. WASHINGTON, D.C. 20024

COVER SHEET FOR TECHNICAL MEMORANDUM

TITLE- The Effect of Asymmetrical IF Filtering on the Envelope of An AM-PDM Waveform

TM- 69-2034-5

DATE- June 30, 1969

FILING CASE NO(S)- 320

AUTHOR(S)- W. D. Wynn

FILING SUBJECT(S)- (ASSIGNED BY AUTHOR(S)-
VHF Communications Systems
Apollo Communications

N79-72769
Unclas
00/32 12714
(NASA-CR-106309) THE EFFECT OF ASYMMETRICAL IF FILTERING ON THE ENVELOPE OF AN AM-RDM WAVEFORM (Bellcomm, Inc.) 55 p

ABSTRACT

A bandwidth incompatibility between the transmitted signal and the receiver of the Apollo VHF communications system has been noted as a possible source of distortion in receiver voice signals. This memorandum investigates the distortion in the demodulated voice waveform introduced by detuning the receiver IF filter from the transmitted carrier frequency. The transmitted signal contains the zero crossings of the voice waveform. Any distortion introduced in the zero crossings prior to the lowpass response of the receiver can result in distortion of the recovered voice. Several test waveforms representing different intensity levels of the voice are processed in a VHF voice system model to determine the effects of asymmetrical IF filtering on the lowpass receiver response. For the test waveforms and system model considered it is concluded that the receiver IF can be detuned as much as 45% of the IF bandwidth before serious distortion appears in the demodulated zero crossings.

X69-19471
(ACCESSION NUMBER) (THRU)
55 2-C
(PAGES) (CODE)
CR-106309 07
(NASA CR OR TMX OR AD NUMBER) (CATEGORY)
FF No. 602(C)
[redacted]

BA-145A (8-68)

EXTRA COPY
CENTRAL FILES

SEE REVERSE [redacted]

BELLCOMM, INC.
955 L'ENFANT PLAZA NORTH, S.W. WASHINGTON, D. C. 20024

SUBJECT: The Effect of Asymmetrical IF Filtering on the Envelope of An AM-PDM Waveform - Case 320

DATE: June 30, 1969

FROM: W. D. Wynn

TM: 69-2034-5

TECHNICAL MEMORANDUM

INTRODUCTION

Frequent periods of distortion and low fidelity have been experienced with the Apollo VHF communications system used to transmit and receive voice signals primarily between the Apollo LM and CSM spacecraft as well as between the Earth and the spacecraft. An incompatibility of the transmitted signal and receiver has been cited since Apollo 7 as a possible source of the distortion. The receiver bandwidths can be as narrow as 60 to 70 KHz while the signal spectrum can occupy 60 KHz or more. Oscillator drifts in the transmitter and receiver along with doppler shift suggest a minimum receiver bandwidth of 80 to 90 KHz for proper operation. This memorandum investigates the distortion of the demodulated voice waveform introduced by detuning the receiver IF filter from the transmitted carrier frequency.

The VHF voice communication system used in the Apollo Program can be modeled by the simplified form shown in Figure 1. A sawtooth clock waveform c is indicated in Figure 1. The minimum of c is zero and the maximum is 2ℓ. The threshold device generates +1 if $c + \nu \geq \ell$ and 0 otherwise. The purpose of c is to guarantee a 50% duty cycle for the transmitter power amplifier when the voice ν is zero.

For a high level voice signal with a variance σ_v^2 that is much larger than ℓ, the effect of c on the system operation is small, and the turn-on and turn-off times of the threshold device, and hence the power amplifier, are approximately the $+\ell$ level crossings of the voice process. If $\sigma_v^2 >> +\ell$ the on-off times of the transmitter will also be approximately the zero crossings of ν. Then in the high level voice signal case the operation of the system approaches that of an infinitely clipped voice system where the information is contained in the zero crossings. For

the case when $\sigma_v^2 \neq o$ but where this variance is not large compared with ℓ, the system in Figure 1 appears impossible to analyze completely for the effect of c and ℓ on the voice intelligibility at the receiver output.

The important question about the system is what effect an asymmetrically tuned band-pass (BP) filter has on the performance of the receiver. A measure of this effect is the distortion induced in m. In the ideal case ($\sigma_v^2 / \ell = \infty$) the envelope E is a pulse train containing the zero crossing information of ν. If σ_v^2 is not large compared to ℓ or if the BP filter distorts s, E gives an incorrect measure of the zeros of ν and hence distortion may be introduced in the demodulated voice.

An analysis is given in this memorandum of the effect of an asymmetrical BP filter on the zero crossings of E and m. This is based on assuming deterministic functions for the threshold output J. The deterministic functions are selected to simulate the small, medium and large σ_v^2 cases in the system. Each deterministic signal J_N is used to define an input $s_n = V J_n \cos\omega_c t$ for the receiver BP filter. The responses r_N, E_N and m_N for each s_n are derived as functions of the asymmetry of the BP filter. The analysis techniques used apply to arbitrary receiver linear BP filters, $H(j\omega)$, and linear low pass filters $L(j\omega)$. However, specific results for r_N, E_N, and m_N are found only for the case

$$H(j\omega) = \begin{cases} k & , \quad \omega_c + \alpha \leq |\omega| \leq \omega_c + \beta \\ 0 & , \quad \text{all other } \omega \end{cases} \tag{1}$$

with

$$(\omega_c + \alpha) > 0;$$

and

$$L(j\omega) = \frac{C}{a + j\omega} \tag{2}$$

If $\alpha = -\beta$, the BP filter has the ideal symmetrical characteristic. As α increases toward zero from the $\alpha = -\beta$ case with $\beta-\alpha$ constant, it can be expected that the distortion in r_N, E_N and m_N increases. The main theme of this report is to discuss this effect and to consider what it infers about distortion of the zero crossings of J.

Additional insight into the system operation follows from the average power spectrum of s_N. From (3-10) in Appendix III the average power spectrum of J_N is

$$|T_n|^2 = \frac{1}{\omega^2} \sum_{n=1}^{N} \sum_{m=1}^{N} \{\cos[n-m]\omega T - 2\cos[n-m-f(m)]\omega T + \cos[n+f(n)-m-f(m)]\omega T\} \tag{3}$$

where $T_n = F[J_N]$. Then the power spectrum of s_N is

$$S_s(\omega) = \frac{1}{2}\left[|T_N|^2_{\omega=\omega+\omega_c} + |T_N|^2_{\omega=\omega-\omega_c}\right] \tag{4}$$

where $\omega = \omega \pm \omega_c$ means ω is replaced by $\omega \pm \omega_c$ in (3).

DISCUSSION

In general the function J is a unit pulse train that can be described by

$$J = \sum_{n=-\infty}^{+\infty} [\underline{u}_1 (t-t_n) - \underline{u}_1 (t-t_n')] \quad , \tag{5}$$

where $t_{n-1} \leq t_{n-1}' \leq t_n \leq t_n$, for every n, and $u_{-1}(t)$ is a unit step function at $t = 0$. The t_n and t_n' are the times of level

ℓ crossings of $\nu + c$. Unless ν is zero, the time sequence $\{t_n, t_n'\}$ is a random process about which very little is known. In a finite interval there will be only a finite number of t_n and t_n'.

In this memorandum a number of finite-duration PDM waveforms are assumed for J. These waveforms are representative of experimental results for J measured over a time interval equal to the inverse of the upper cutoff frequency f_{co} of ν. The waveforms are assumed as models of J for $\sigma_v^2 << \ell$, $\sigma_v^2 \sim \ell$ and $\sigma_v^2 >> \ell$ over a time interval in which ν makes a positive and a negative zero crossing. These waveforms are described by

$$J_N = \sum_{n=1}^{N} [\underline{u}_1 (t-nT) - \underline{u}_1 [t-(n+f(n))T]] \qquad (6)$$

where $NT \sim 1/f_{co}$. If N and T are specified the behavior of J_N depends completely upon f(x) where $0 \leq f(x) \leq 1$, as pointed out in Appendix II. This f(x) limits J_N to a sequence of unit amplitude pulses of duration f(n)T where n = 1,2...,N. The sum (6) is more restricted than the sum of terms for n = 1,2...,N in (5), since $t_n = nT$ are known times spaced T apart. The only variation in the N pulses of (6) comes from f(x).

If $\nu \equiv 0$ the function J is a sequence of equally spaced unit pulses each of duration T/2. In (6), N cycles of this periodic function are obtained if f(x) = 1/2 for all x. If f(x) = 1 for $t_a \leq x \leq t_b$ where t_a and t_b belong to the interval [T,(N+1)T] and if f(x) = 0 for all other x, the corresponding J_N is a single square pulse in the interval [T,(N+1)T].

Four cases of f(x) were considered. These are the piecewise linear functions shown in Figure 2. In each case $0 \leq f(x) \leq 1$. The functions J_N and s_N corresponding to $f_i(x)$ with i = 1,2,3,4 are J_{Ni} and s_{Ni}, respectively. The J_{Ni} and

s_{Ni} are representative of J_N and s_N in an interval $[T,(N+1)T]$ with $NT \sim 1/f_{co}$, where σ_v^2/ℓ increases from less than unity (Case I) to $\sigma_v^2/\ell = \infty$ (Case IV).

From (1-8) in Appendix I the response of the BP filter (1) to $s_N = V\, J_N \cos \omega_c t$ is

$$r_N = V\, R_e \left\{ e^{j\omega_c t}\, F^{-1} [H_{\ell_1}(j\omega) \cdot F(J_N)] \right\} \tag{7}$$

where

$$H_{\ell_1}(j\omega) = H(j\omega + j\omega_c)\, u_{-1}(\omega + \omega_c) \tag{8}$$

is the lowpass equivalent filter for $H(j\omega)$, F^{-1} denotes the inverse Fourier transform, and R_e means the real part.

For the J_N function (6), (7) follows in (2-10) of Appendix II. From (2-10) the envelope E_N in Figure 1 is

$$E_N = \frac{kV}{2\pi} \left[\left(\sum_{n=1}^{N} X_n \right)^2 + \left(\sum_{n=1}^{N} Y_n \right)^2 \right]^{1/2} \tag{9}$$

The X_n and Y_n are combinations of the tabulated functions $S_i(y_n)$ and $C_i(y_n)$ where y_n depends upon $f_i(x)$, α, β, n, T and t.

The response of $L(j\omega)$ in (2) is the convolution

$$m_N = \int_{-\infty}^{+\infty} \ell(t-x)\, E_N(x)\, dx \quad , \tag{10}$$

where $\ell(t) = F^{-1}[L(j\omega)]$. For the cases of f(x) in Figure 2, the responses E_{Ni} in (9) are very complicated. To obtain m_{Ni} in (10) the Fast Fourier Tranform (FFT) computer algorithm was used to perform the convolution.

RESULTS

The functions J_N, E_N and m_N are computed for t in the interval [T,(N+1)T] using equations (6), (9) and (10), respectively. Also, the power spectrum in (3) is computed in the frequency interval where $|T_N|^2$ is of significance. A collection of graphs of (3), (6), (9) and (10) are given for each $f_i(x)$, i = 1,2,3 and 4, where the amount of asymmetry in the receiver BP filter is varied discretely. The results are obtained for the numerical values:

(i) $\beta - \alpha = 75$ KHz.

(ii) α = Discrete values between -37.5 KHz and 0.

(iii) N = 30.

(iv) $T = 0.333 \times 10^{-4}$ seconds.

(v) In (2), $a = 18\pi \times 10^3$ and C = 1.

(vi) In (9), $\frac{kV}{2\pi} = 1$ to normalize E_N.

For these values the sawtooth clock has a frequency of 30 KHz and the voice $f_{co} \sim 10^3$ Hz. The graphs are divided into the cases I through IV for f(x) in Figure 2. In each case values of α are selected in the range (ii). Figures 3 through 6 are the graphs of J_N for f(x) in cases I through IV, respectively. Figures 7 through 18 are the graphs of the power spectra of J_N for the four cases of f(x). For clarity three spectra are given in each case; the complete spectra, the low frequency portion, and the high frequency portion. The intermediate and lowpass frequency functions E_N and m_N for $-\alpha$ = 37.5, 25.5, 13.5, 6, 4, 2, 1 and 0 KHz are shown in Figures (19) through (34).

CONCLUSIONS

In each of the four cases the lowpass filter response m_N retains the same general shape for α between -37.5 KHz and -4 KHz. The envelope E_N and the high frequency content of $m_N(t)$ vary considerably with changes in α between -37.5 KHz and 0. The desired voice information is contained in the zero crossings which are transmitted with varying degrees of error by the pulse edges of E and m. The positions and slopes of the edges of m_N are part of the low frequency information in m_N that does not vary as α changes in the interval -37.5 KHz to -4 KHz. From these results it is concluded that detuning the IF filter of the receiver has little effect on the zero crossing estimates of the voice carried in m if the filter passes the part of the signal spectrum around ± 4 KHz of the carrier. Then the receiver IF may be detuned by as much as 45% of the IF bandwidth before the zero crossing information contained in m is distorted appreciably.

W. D. Wynn

2034-WDW-ulg

W. D. Wynn

Attachments
Figures 1-35
Appendices I-III

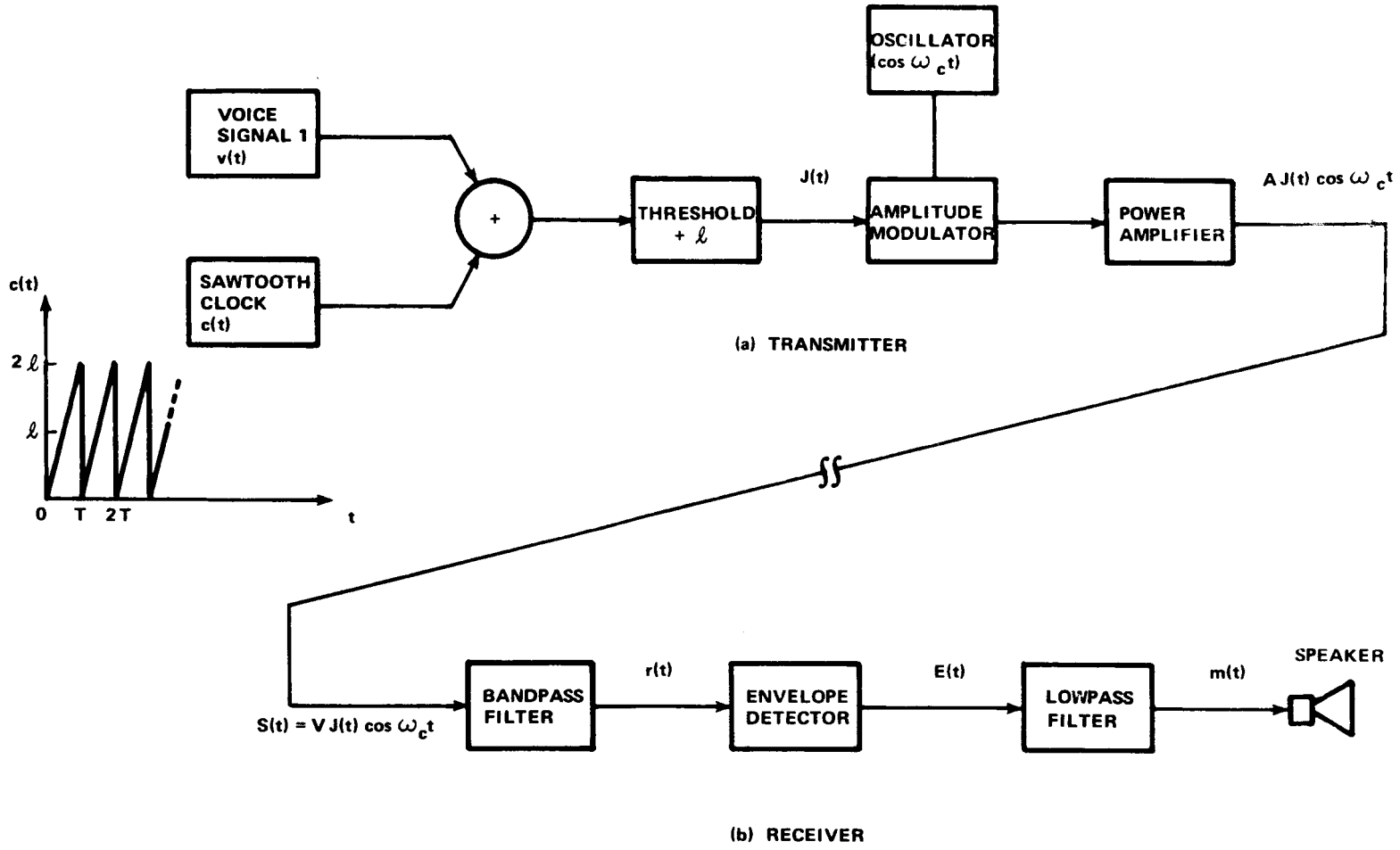

FIGURE 1 - A SIMPLIFIED MODEL OF A VHF VOICE COMMUNICATION SYSTEM

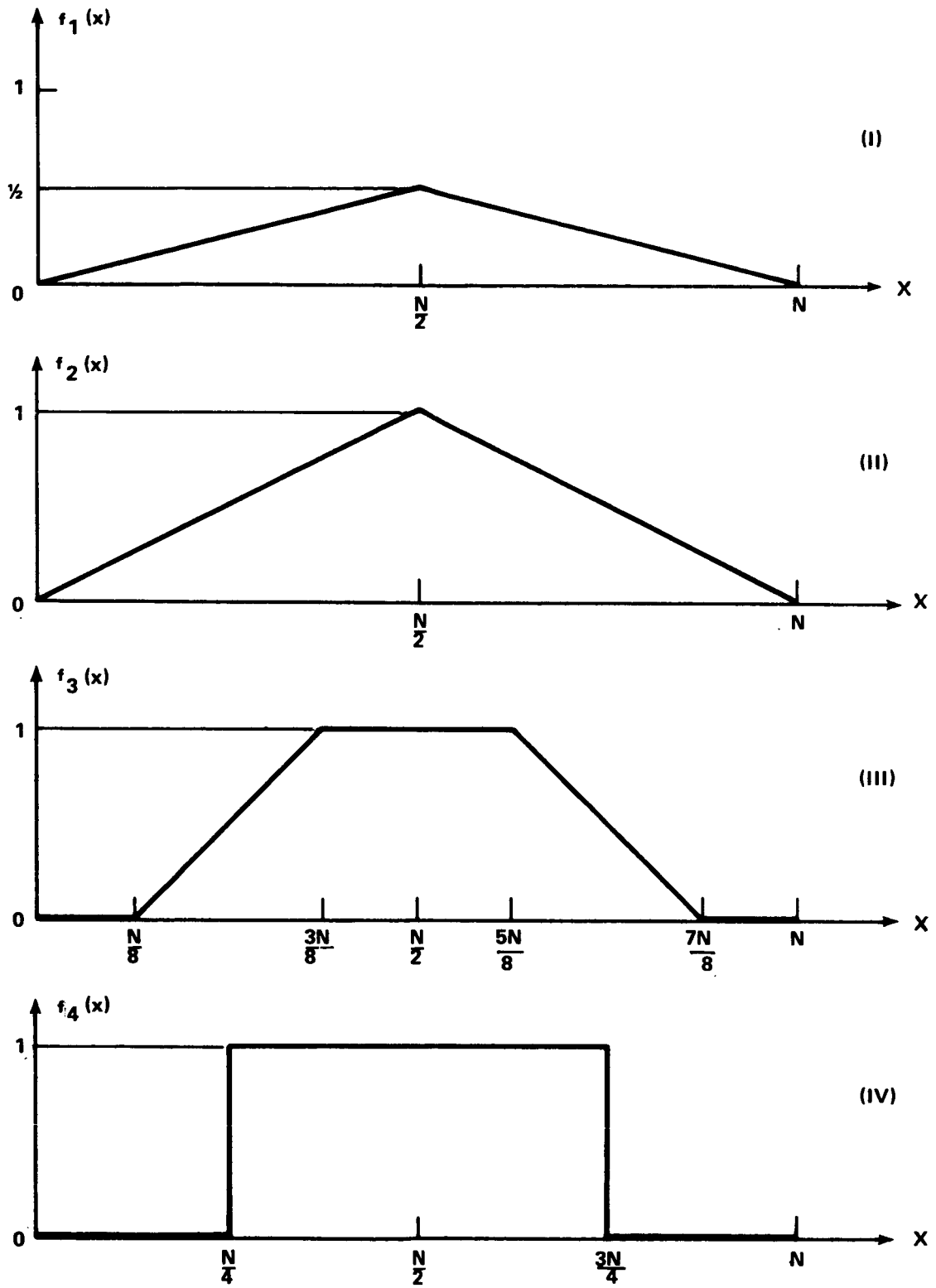

FIGURE 2 - CASES OF f(x) FOR THE J_N (t) FUNCTION

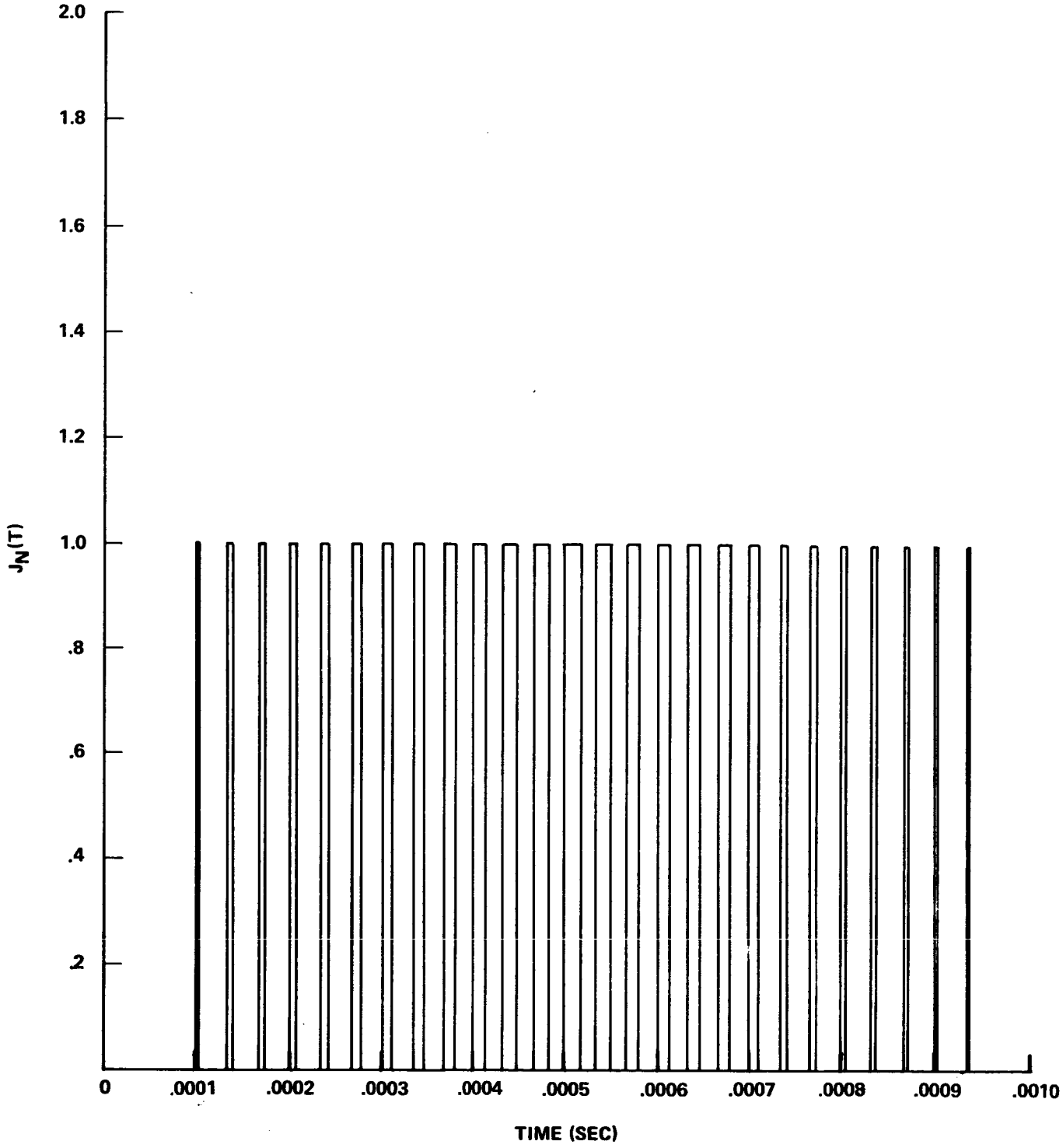

FIGURE 3- FUNCTION J_N FOR f (x) IN CASE I

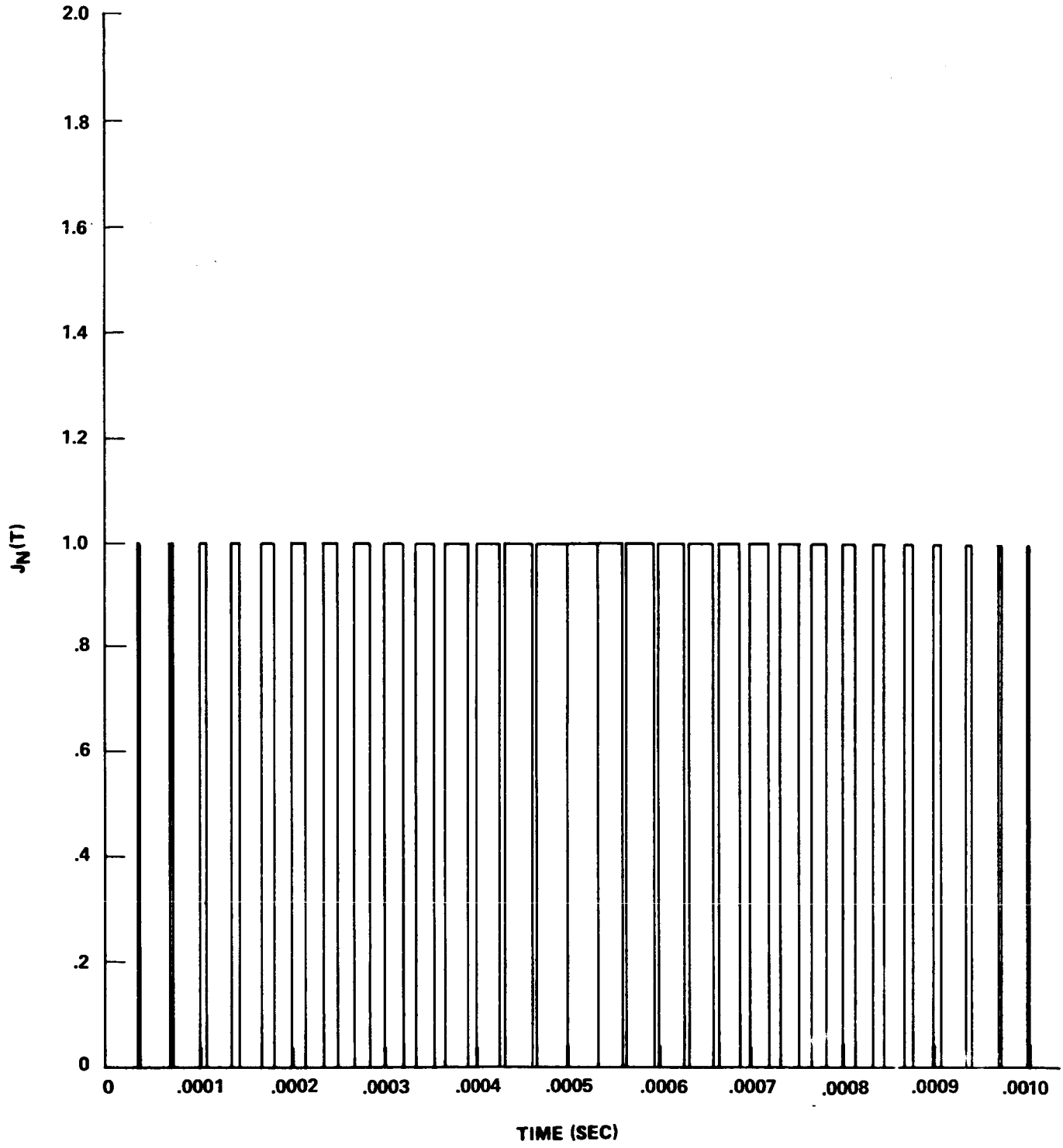

FIGURE 4 - FUNCTION J_N FOR f(X) IN CASE II

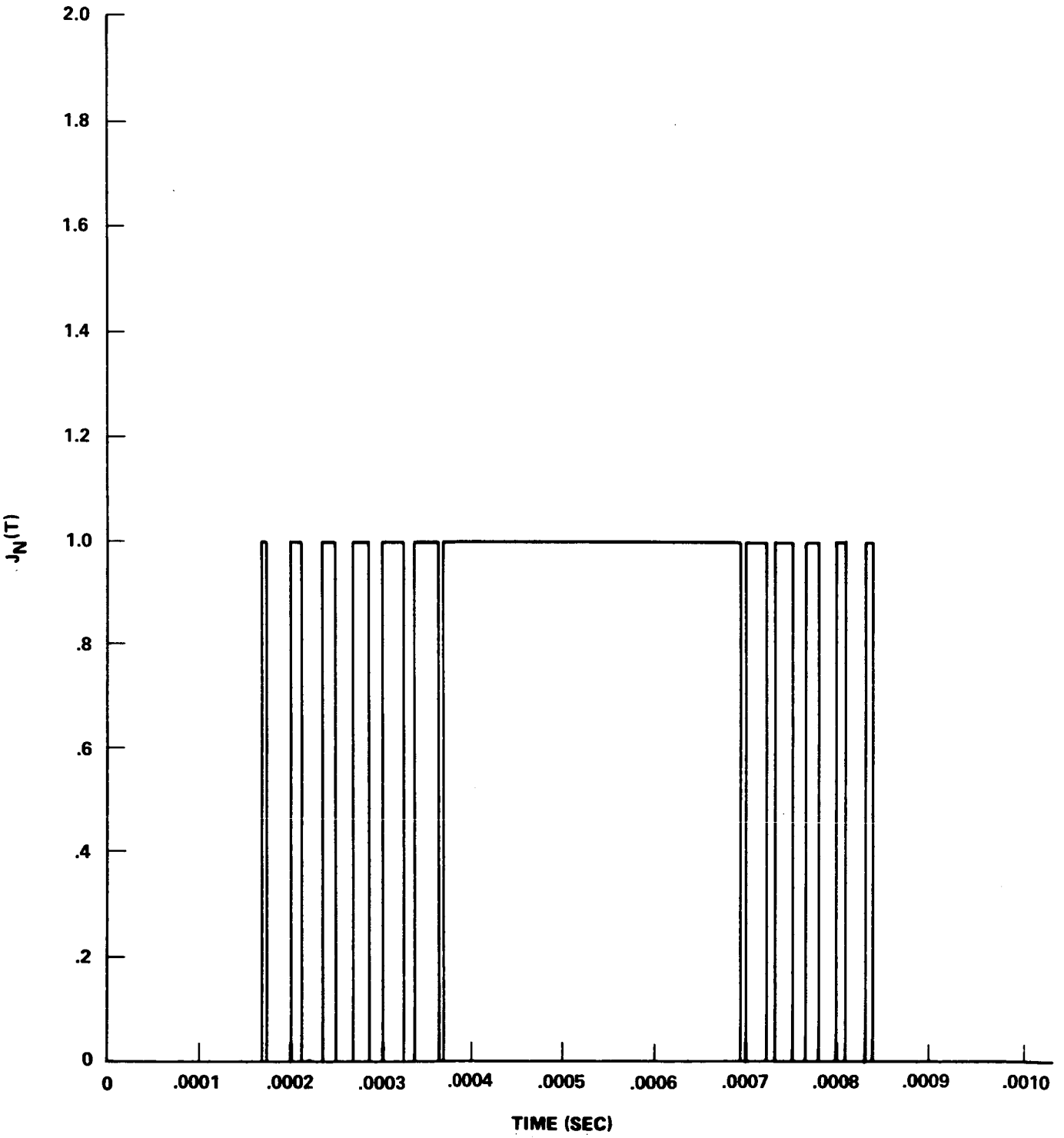

FIGURE 5 - FUNCTION J_N FOR f (x) IN CASE III

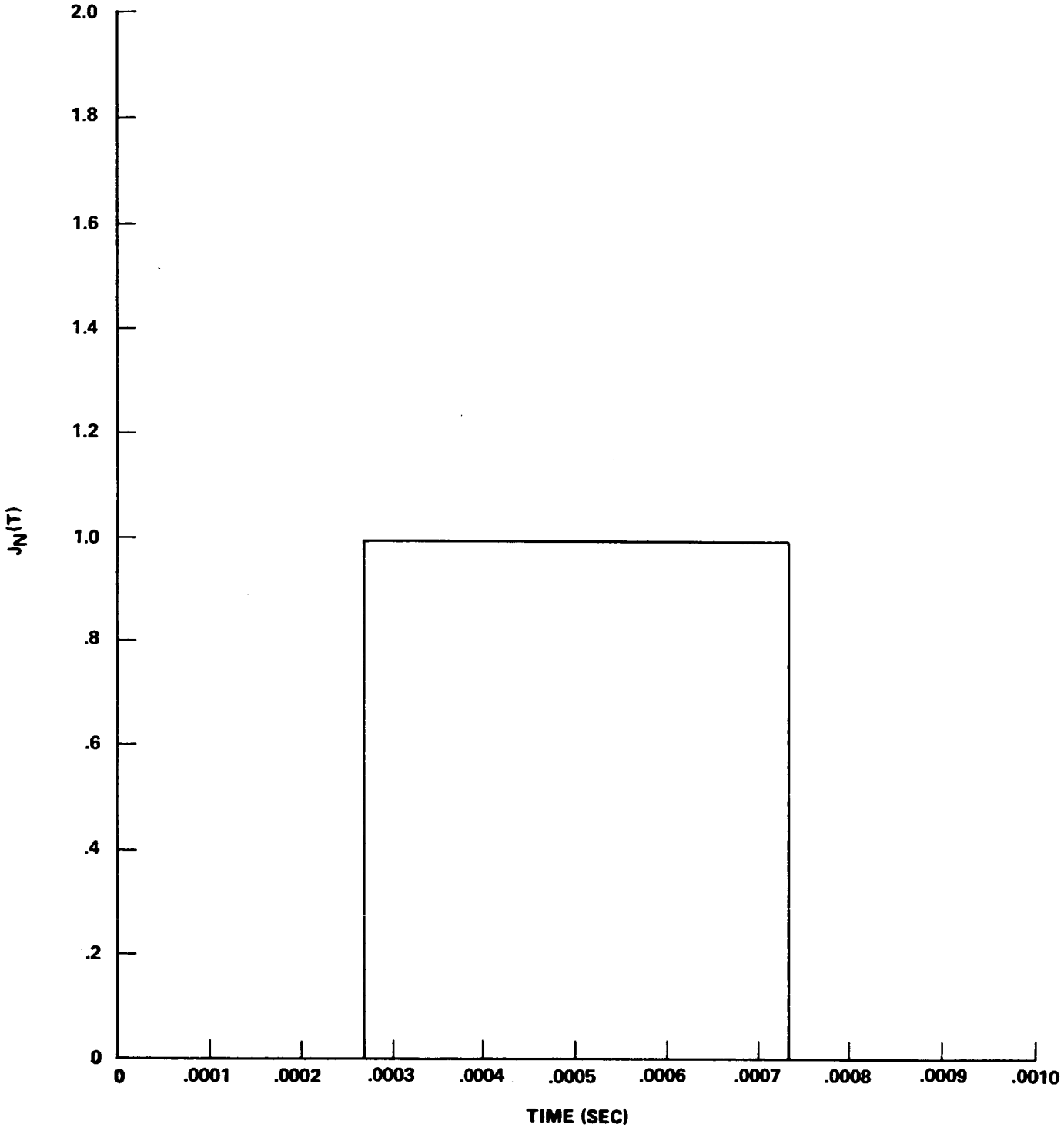

FIGURE 6 - FUNCTION J_N FOR f (x) IN CASE IV

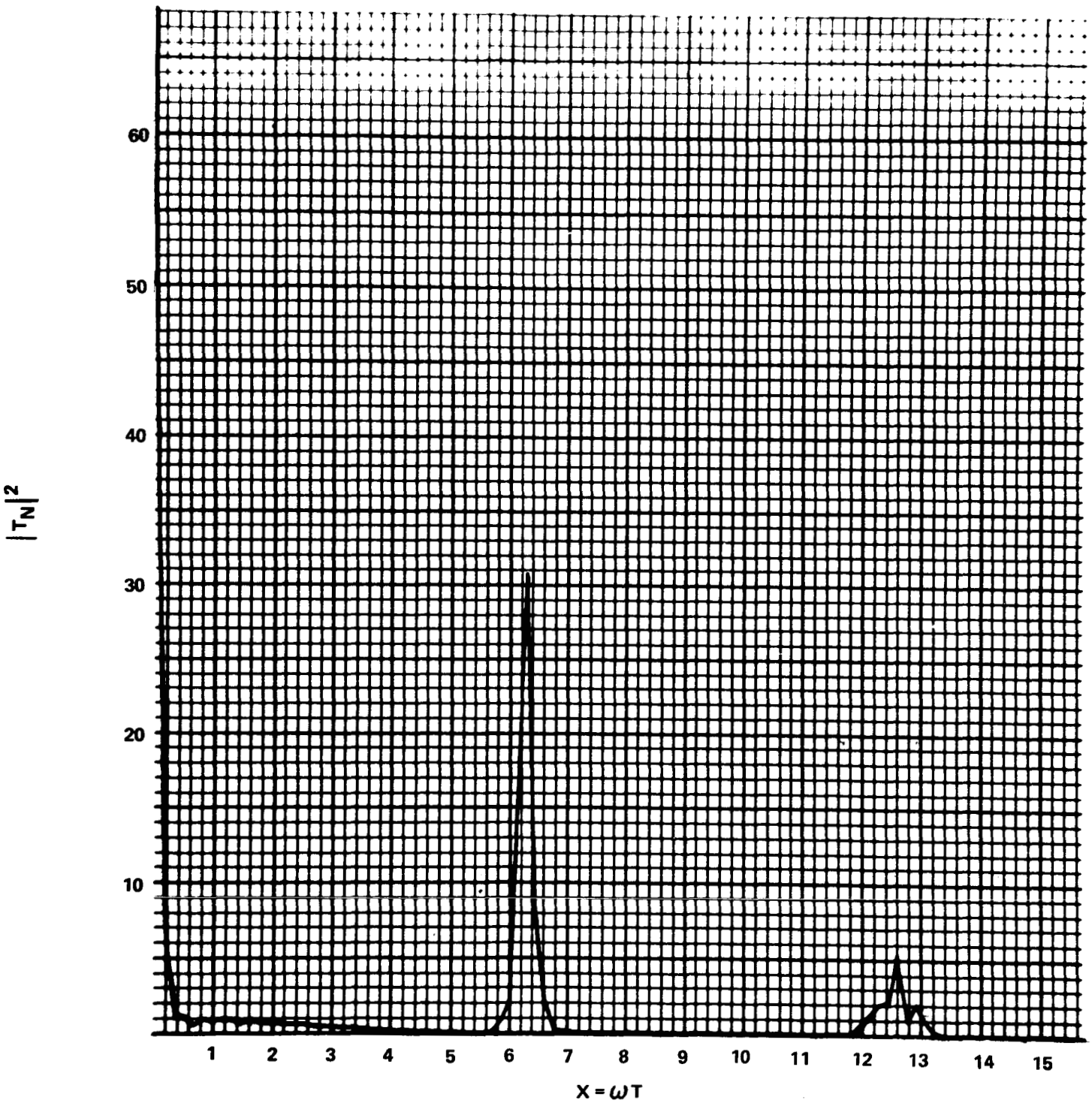

FIGURE 7 - THE POWER SPECTRUM OF J_N FOR f (x) IN CASE I

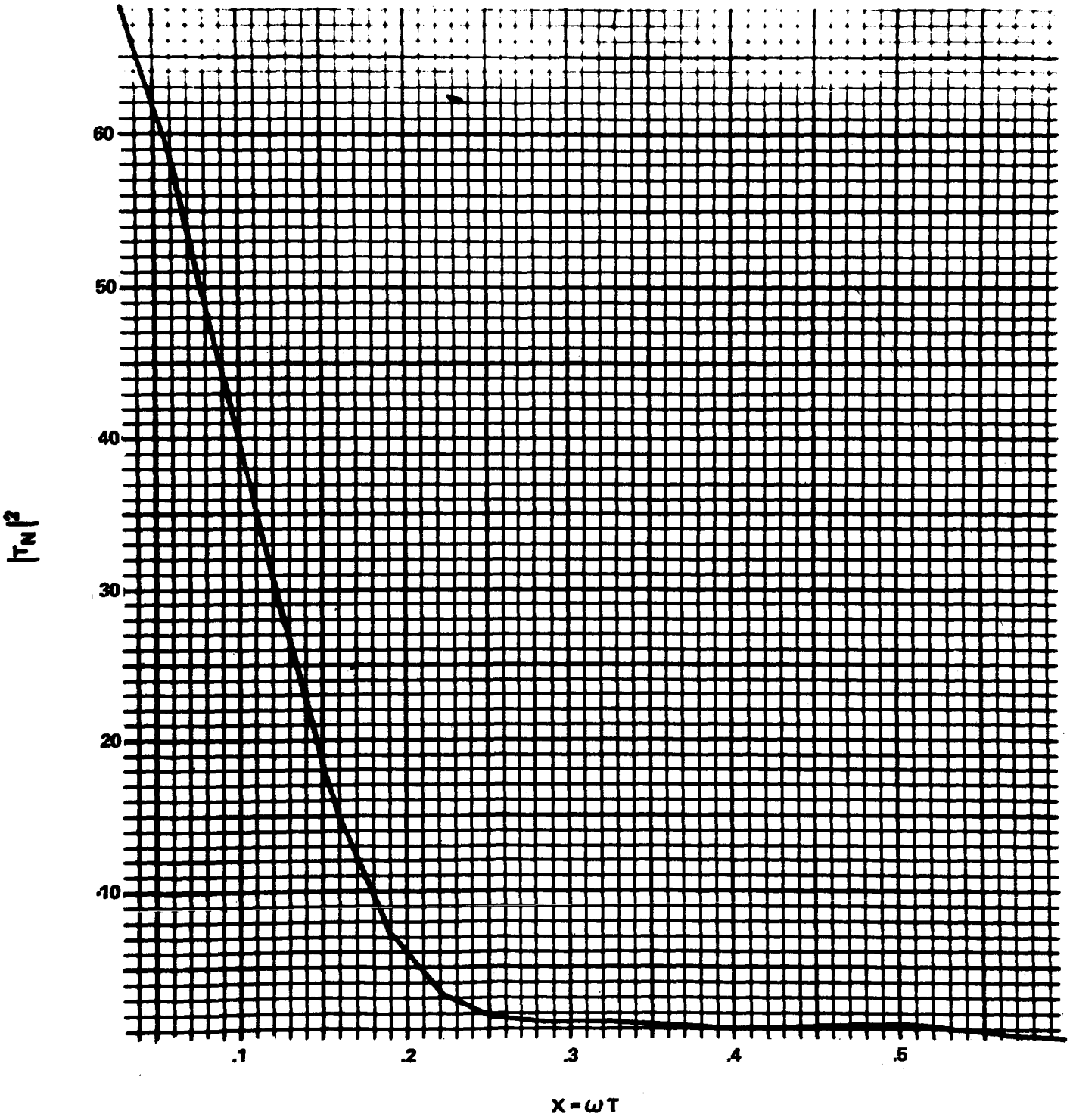

FIGURE 8 - THE POWER SPECTRUM OF J_N FOR f (x) IN CASE I

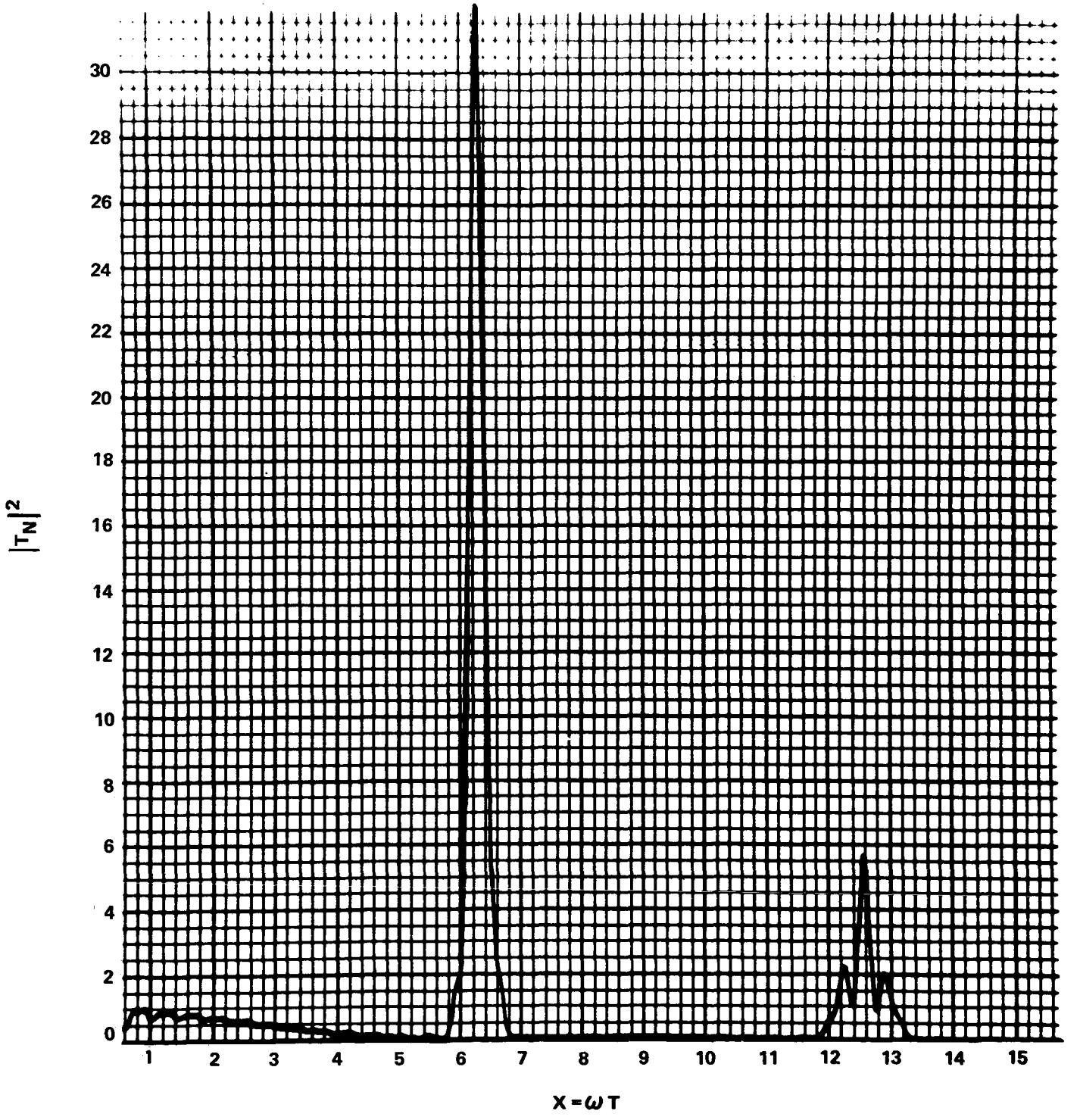

FIGURE 9 - THE POWER SPECTRUM OF J_N FOR f (x) IN CASE I

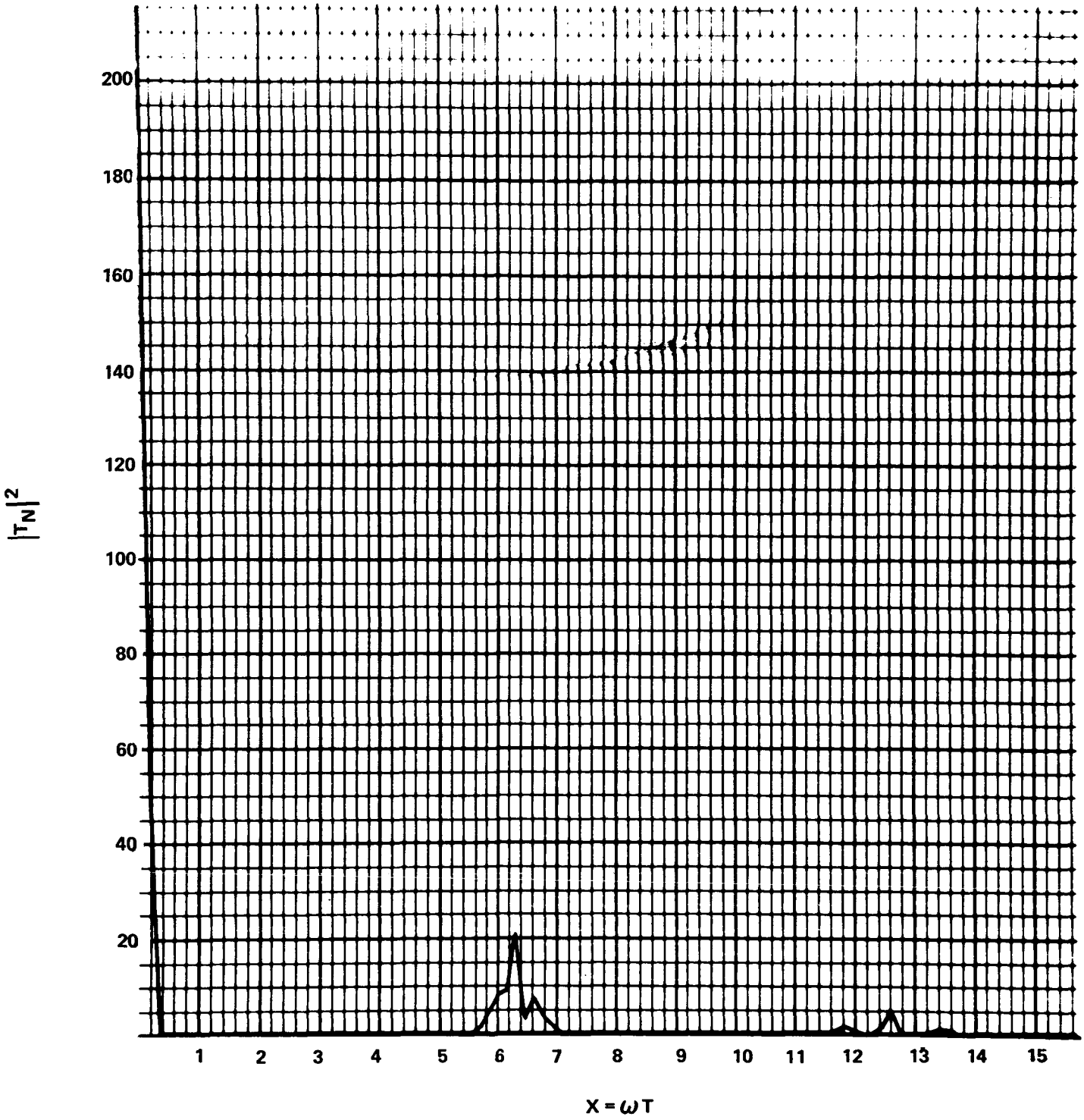

FIGURE 10 - THE POWER SPECTRUM OF J_N FOR f (x) IN CASE II

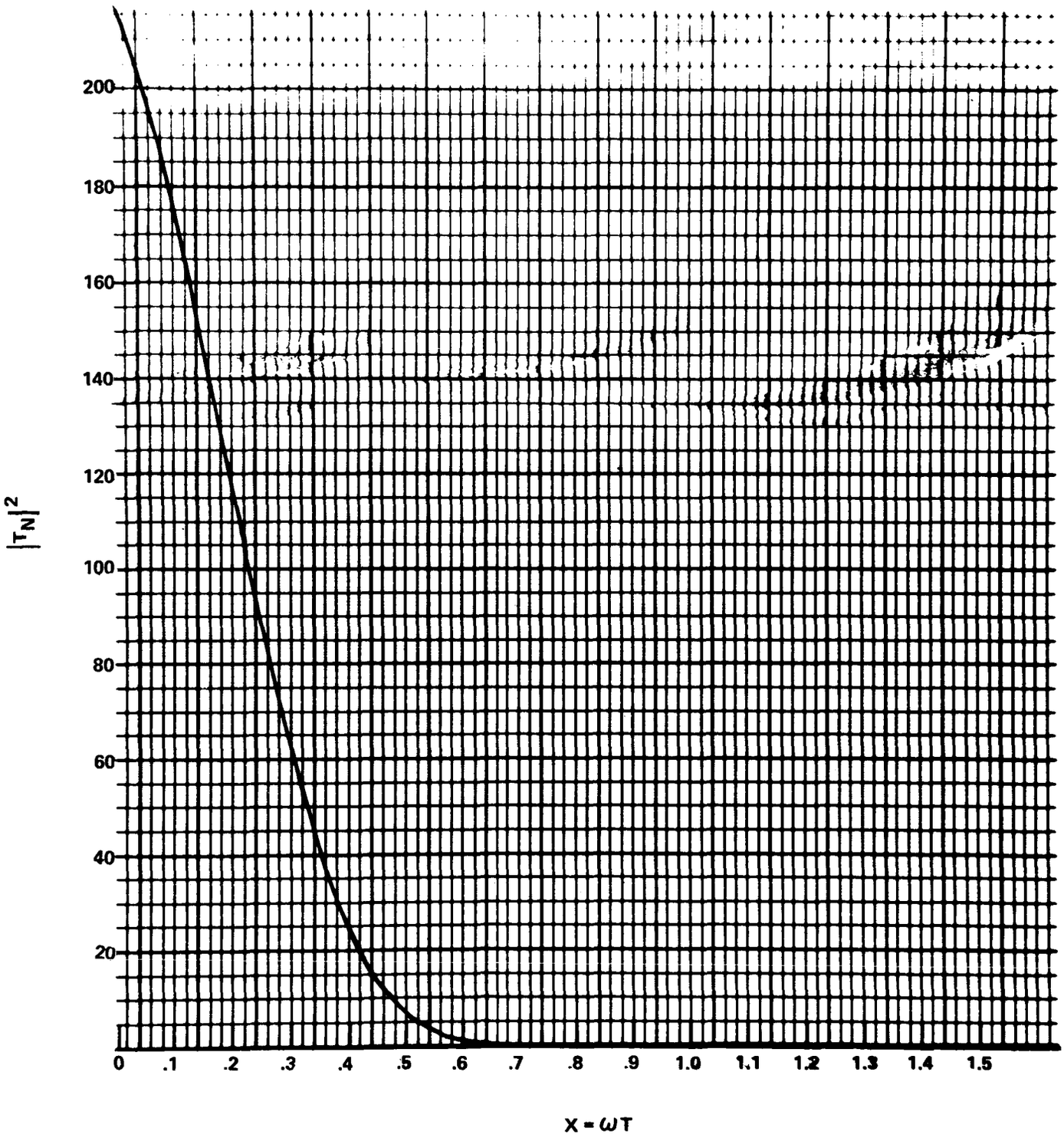

FIGURE 11 - THE POWER SPECTRUM OF J_N FOR f (x) IN CASE II

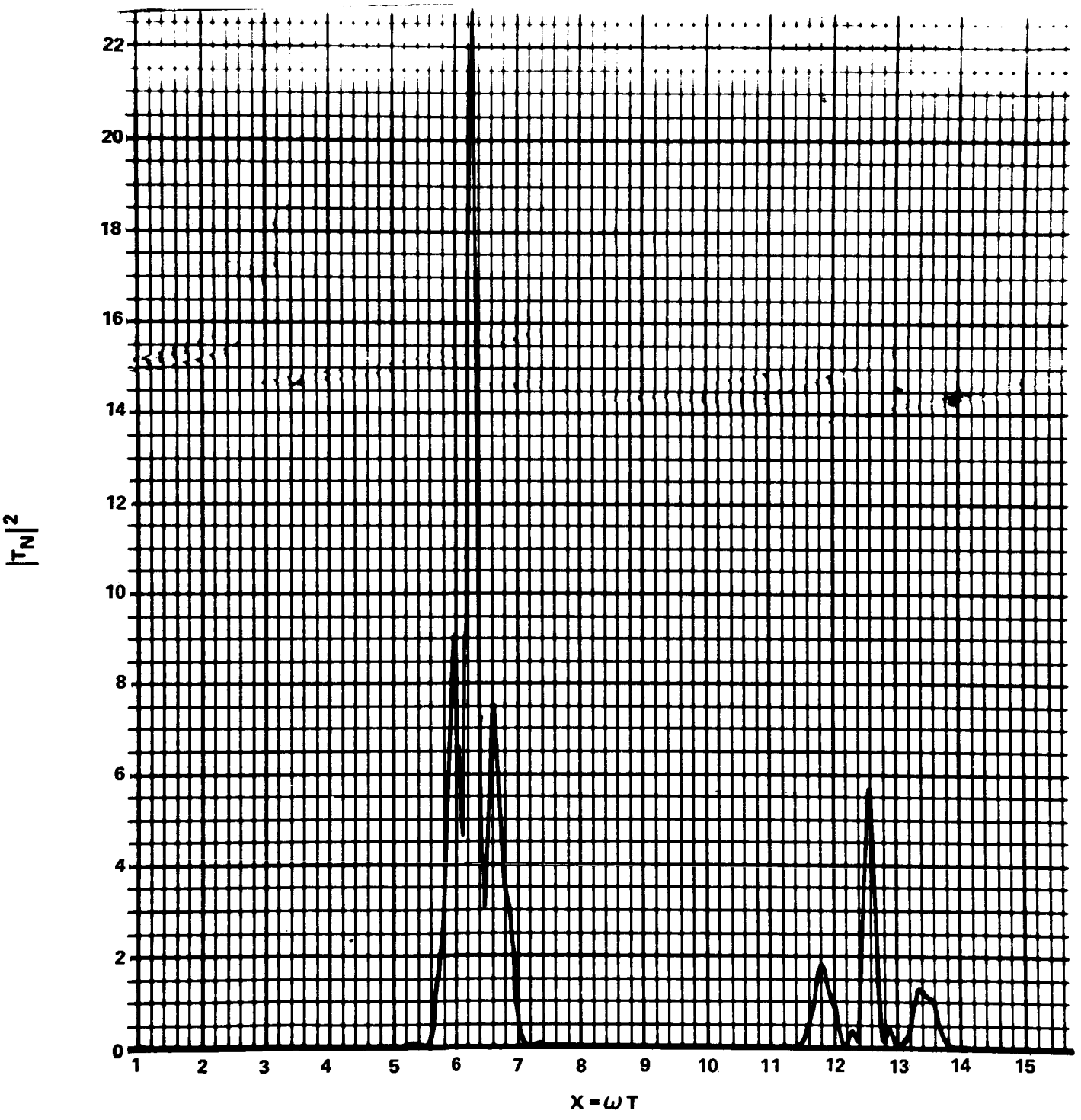

FIGURE 12 - THE POWER SPECTRUM OF J_N FOR F(x) IN CASE II

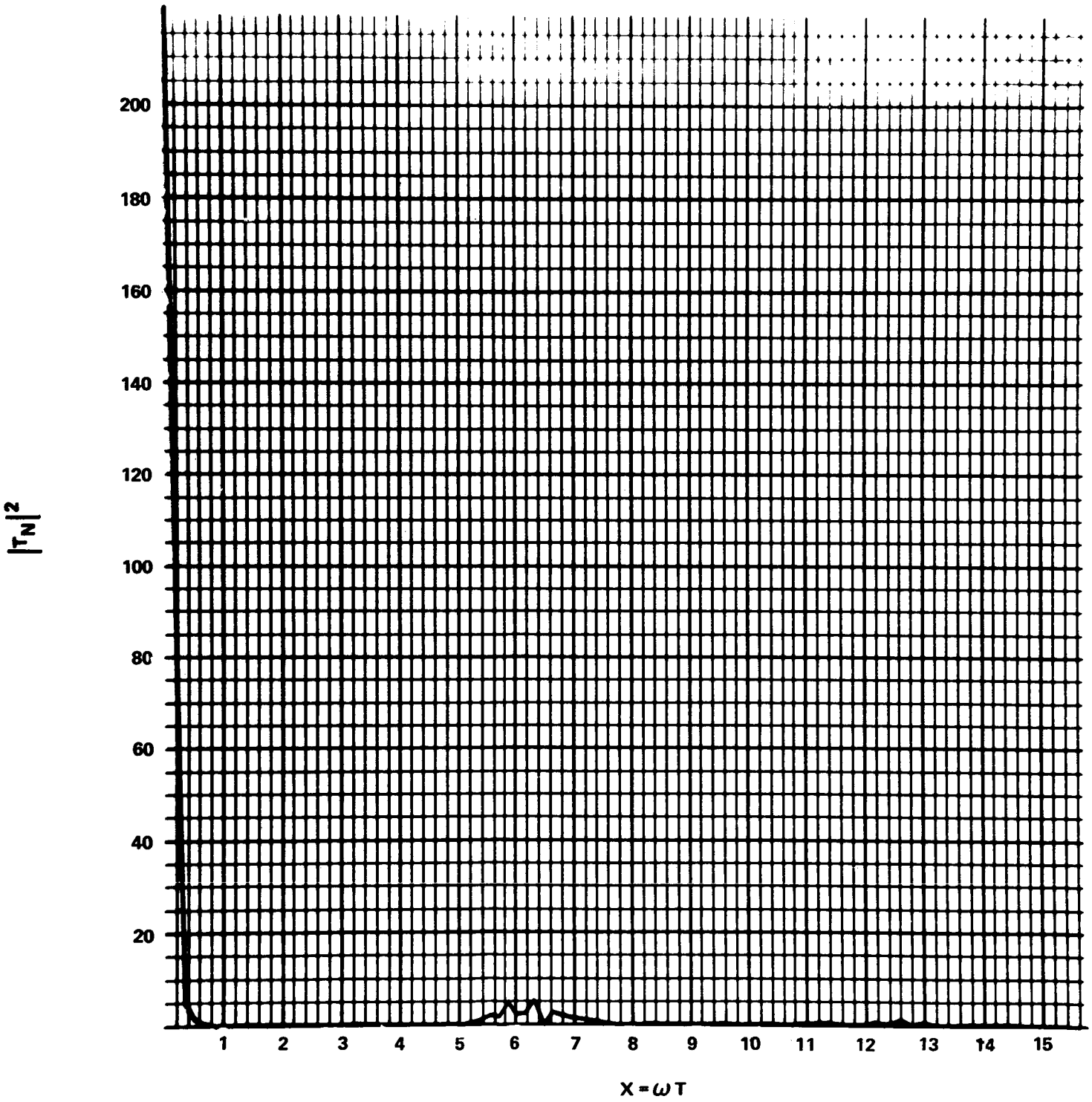

FIGURE 13 - THE POWER SPECTRUM OF J_N FOR f (x) IN CASE III

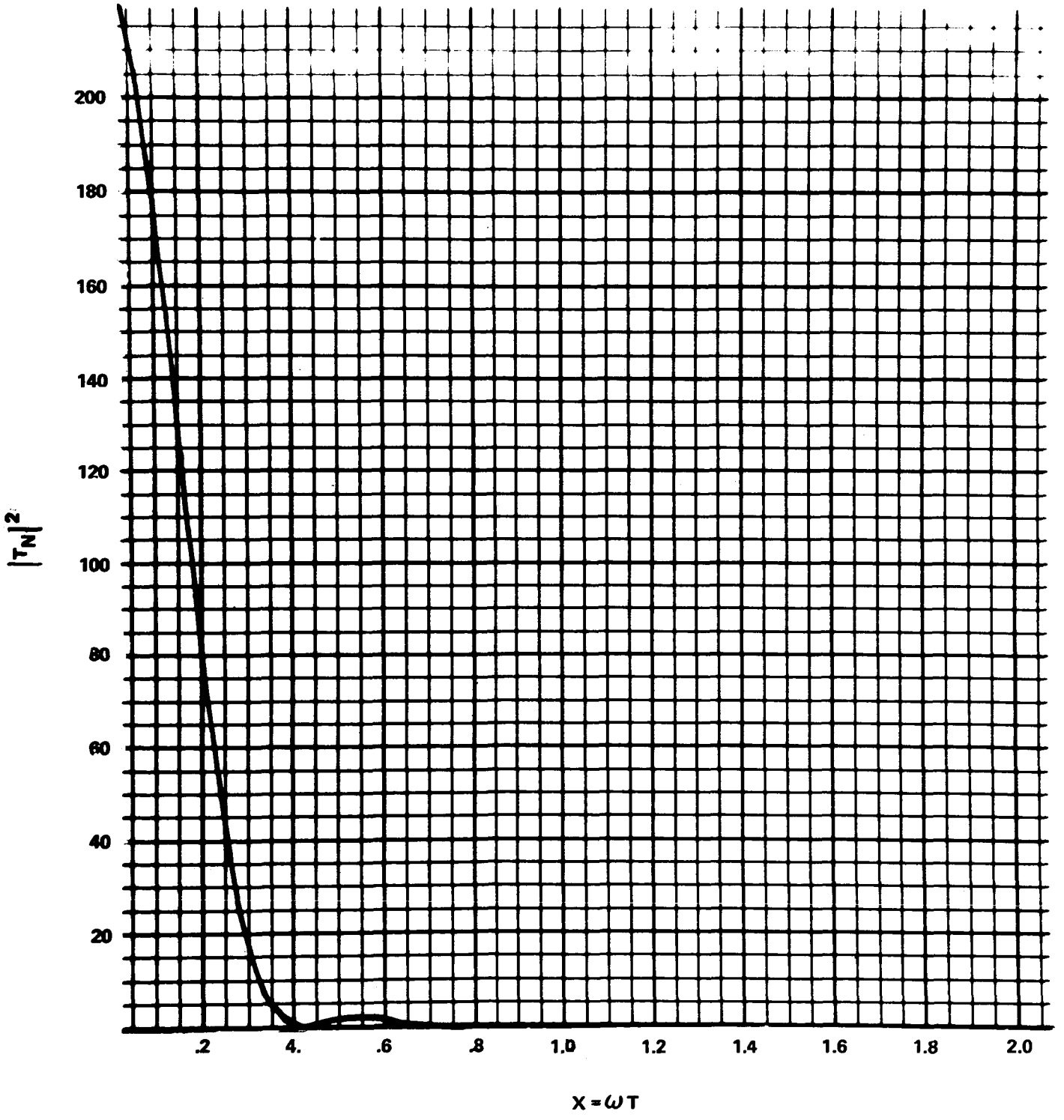

FIGURE 14 - THE POWER SPECTRUM OF J_N FOR f (x) IN CASE III

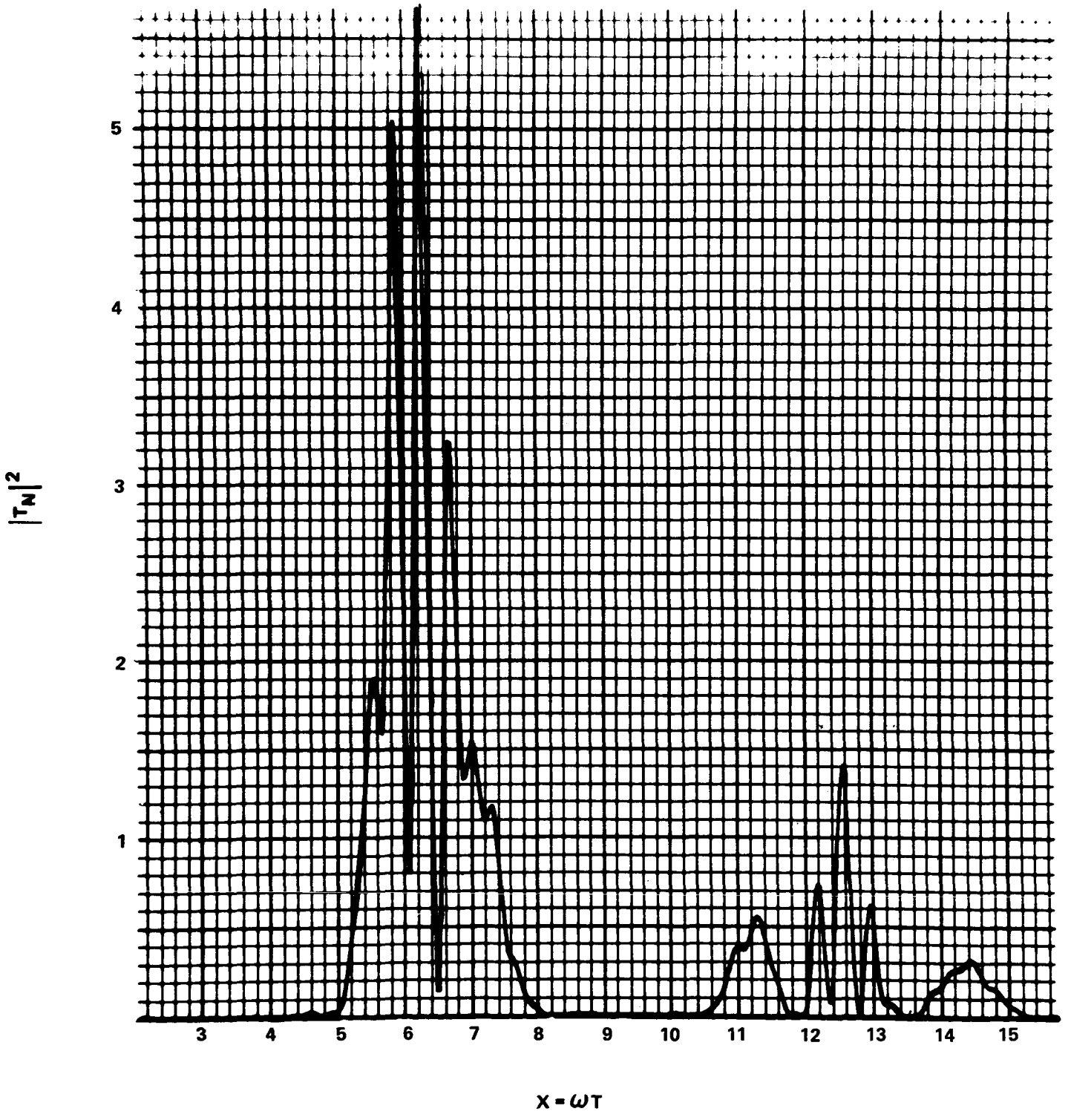

FIGURE 15 - THE POWER SPECTRUM OF J_N FOR f (x) IN CASE III.

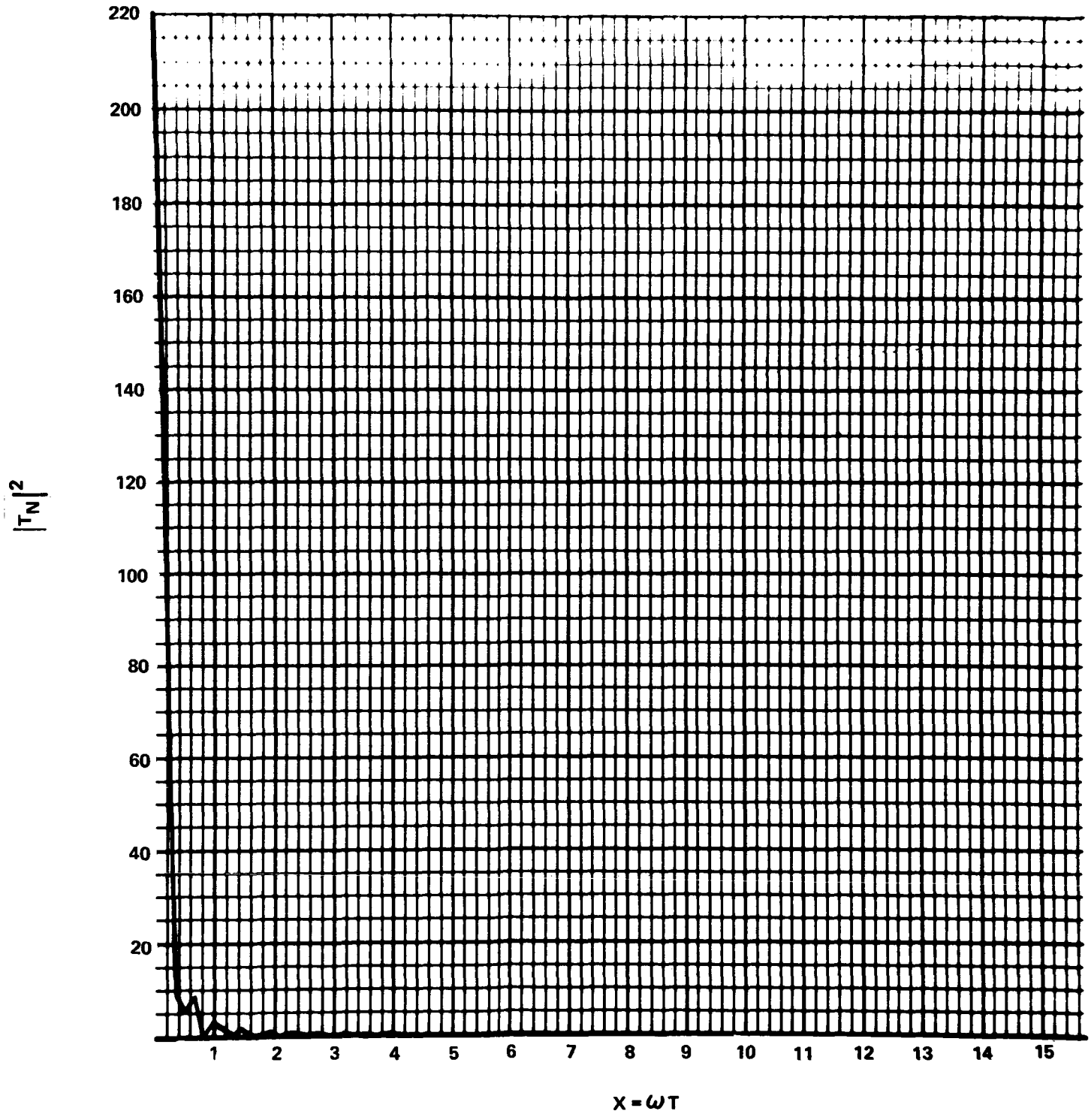

FIGURE 16 - THE POWER SPECTRUM OF J_N FOR f(x) IN CASE IV

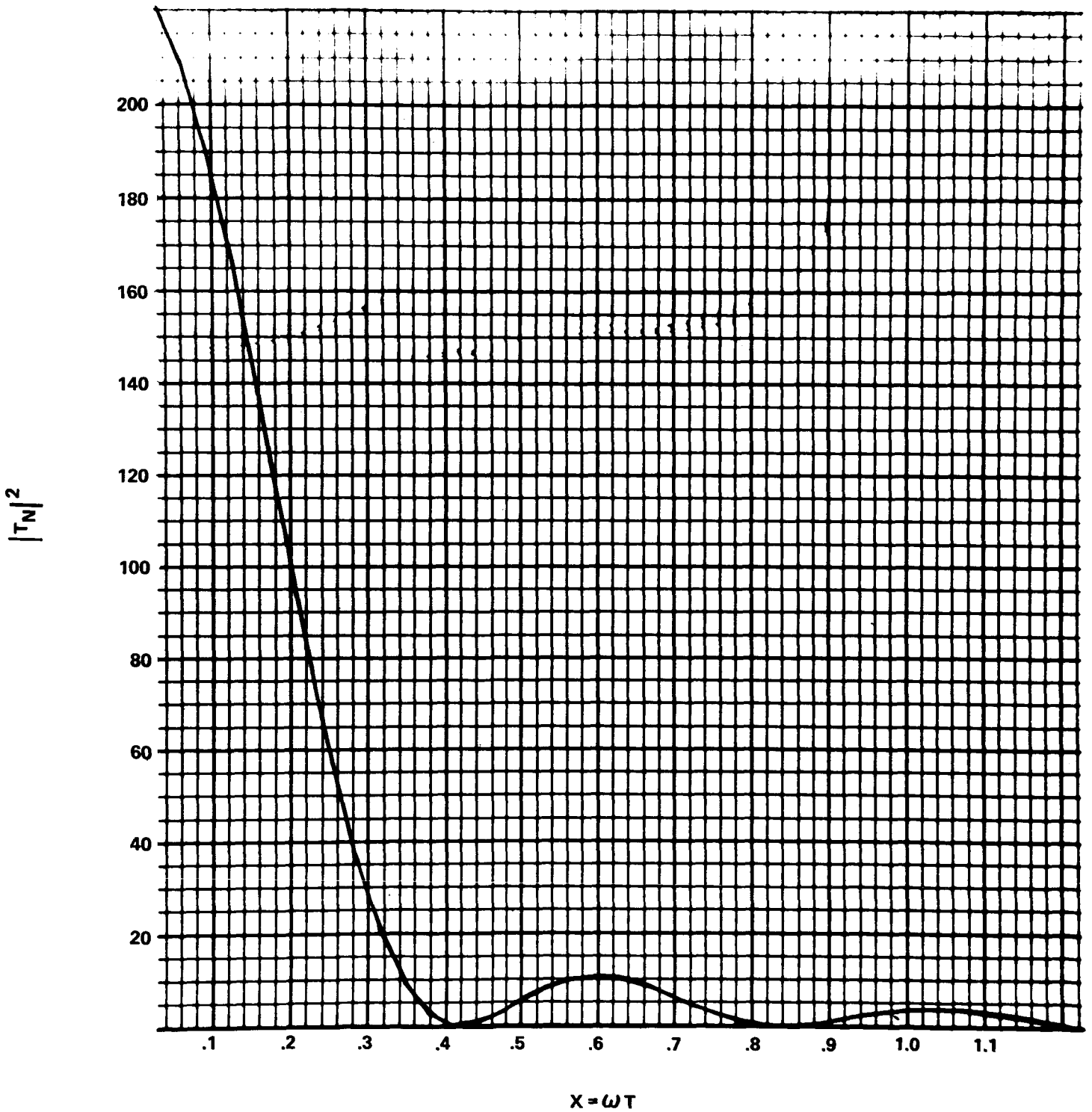

FIGURE 17 - THE POWER SPECTRUM OF J_N FOR f (x) IN CASE IV

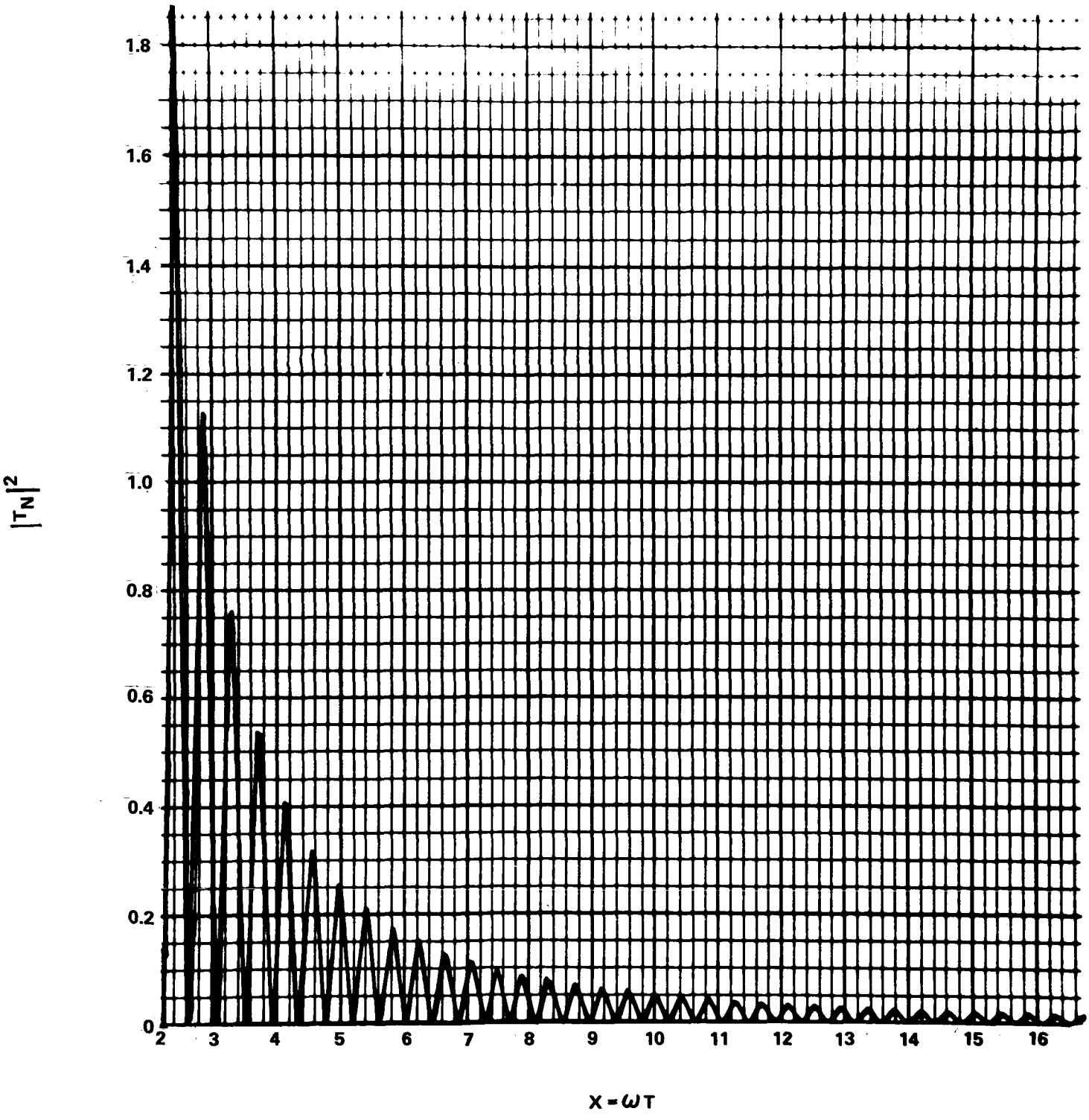

FIGURE 18 - THE POWER SPECTRUM OF J_N FOR f (x) IN CASE IV

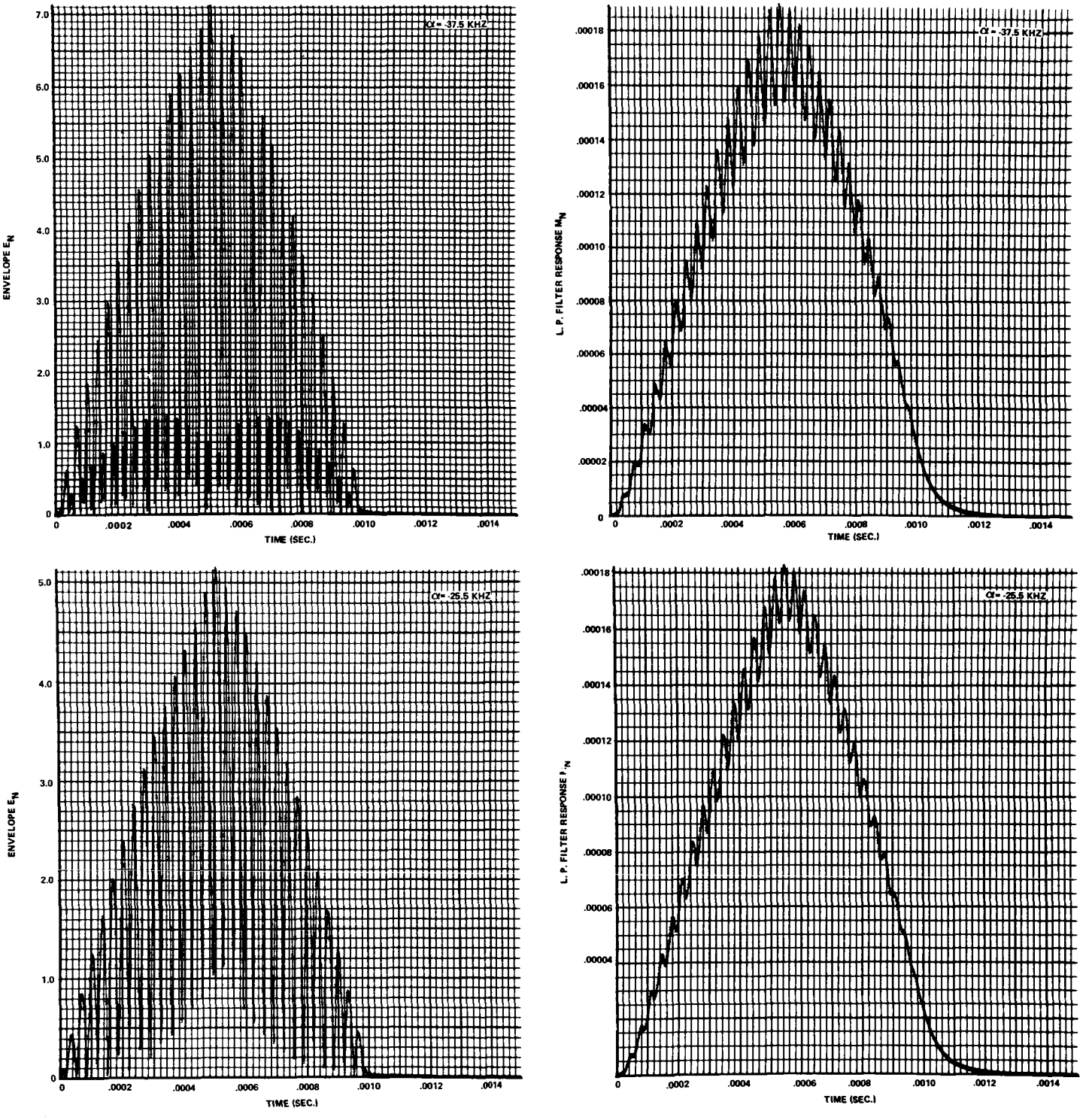

FIGURE 19 GRAPHS OF E_N AND M_N FOR CASE I

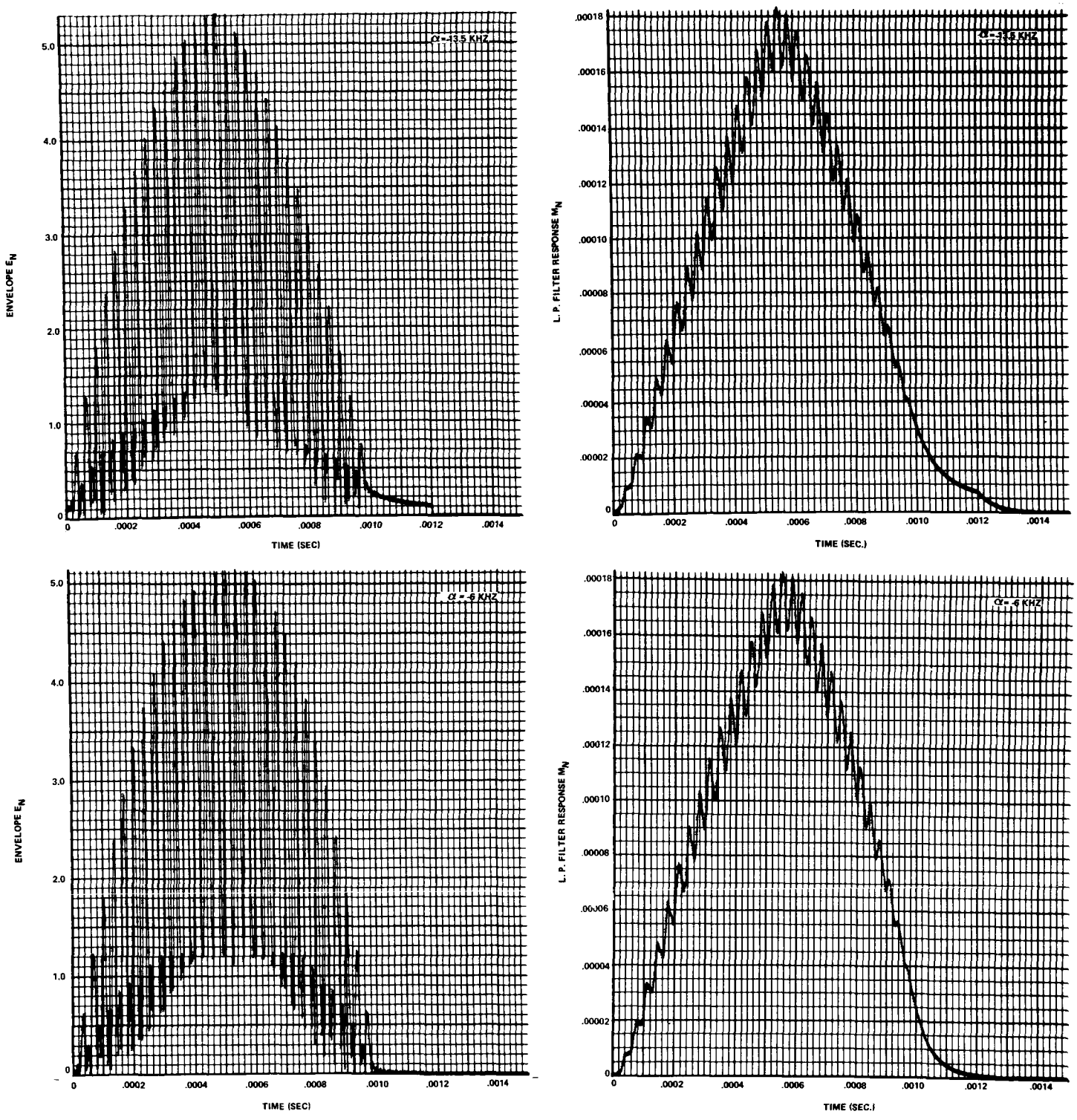

FIGURE 20-GRAPHS OF E_N AND M_N FOR CASE I

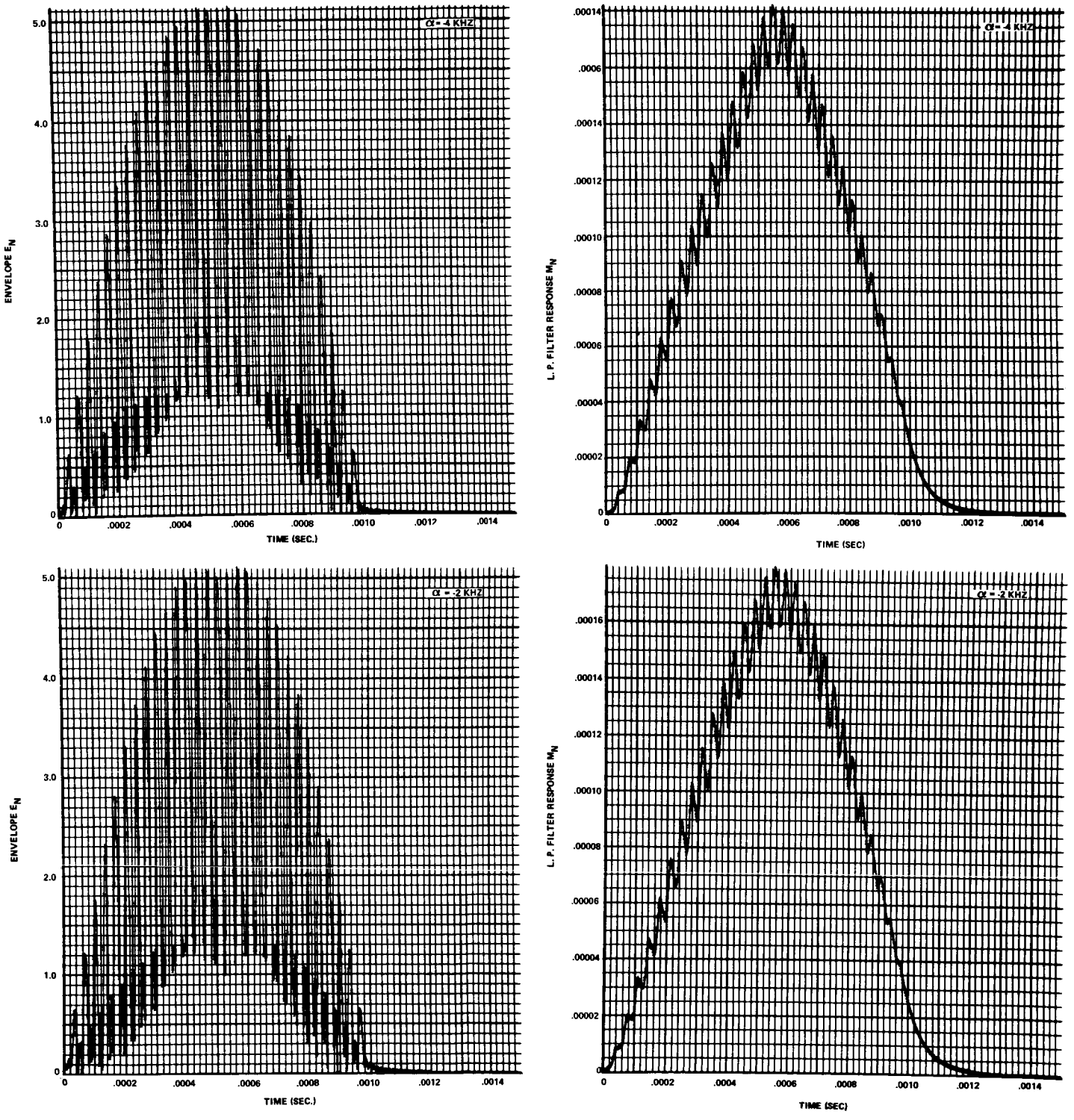

FIGURE 21-GRAPHS OF E_N AND M_N FOR CASE I

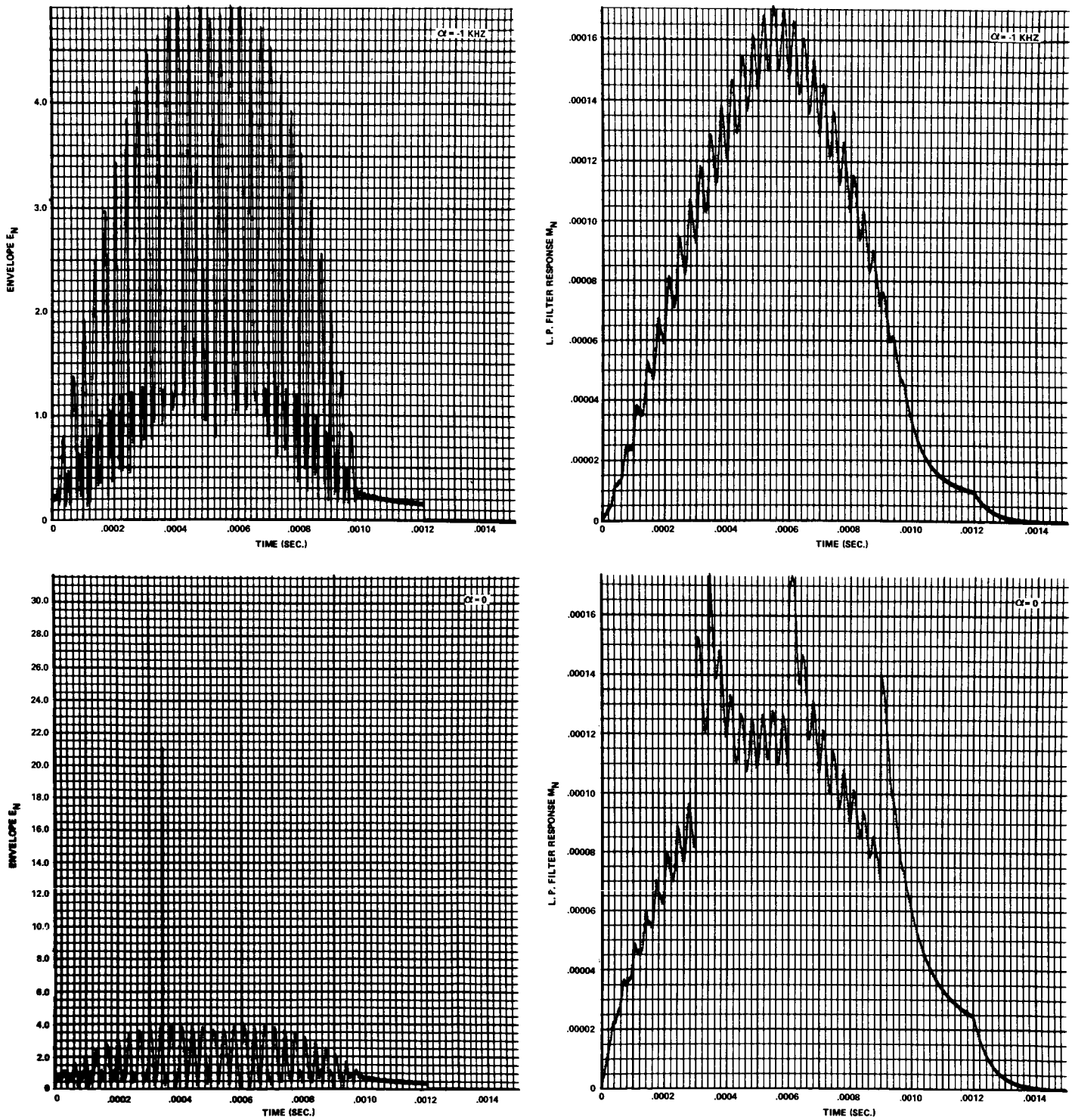

FIGURE 22-GRAPHS OF E_N AND M_N FOR CASE I

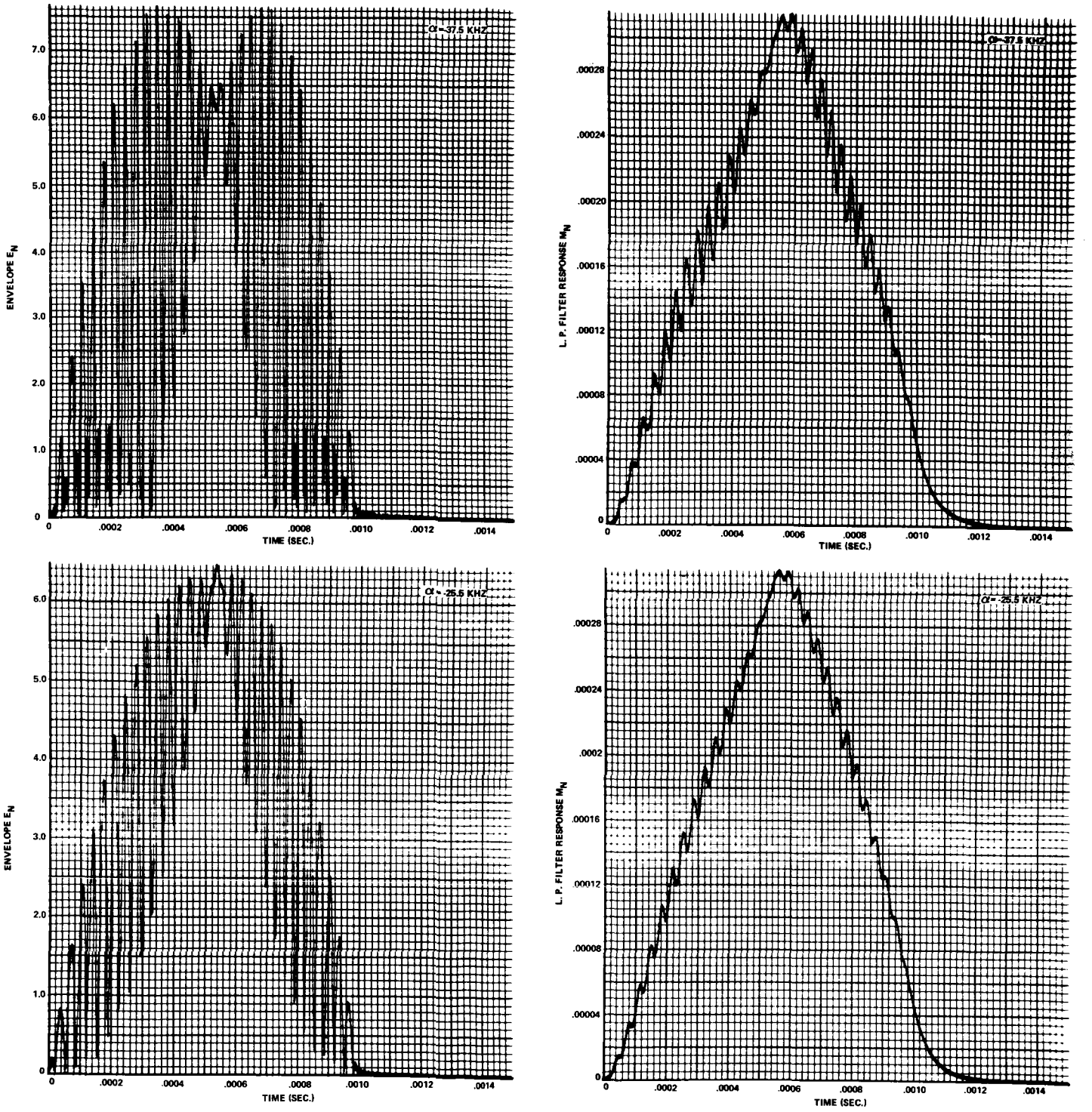

FIGURE 23 - GRAPHS OF E_N AND M_N FOR CASE II

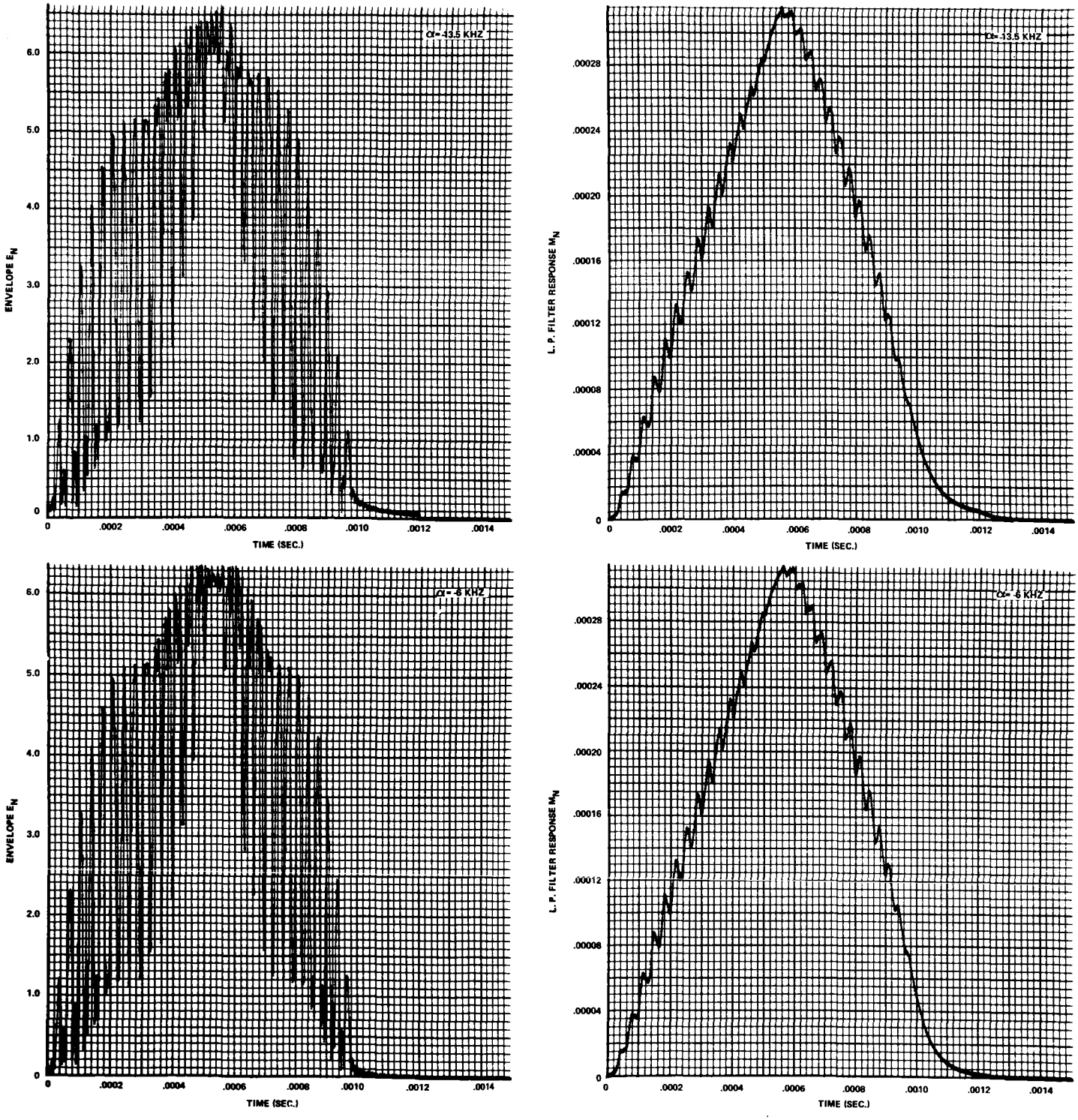

FIGURE 24 GRAPHS OF E_N AND M_N FOR CASE II

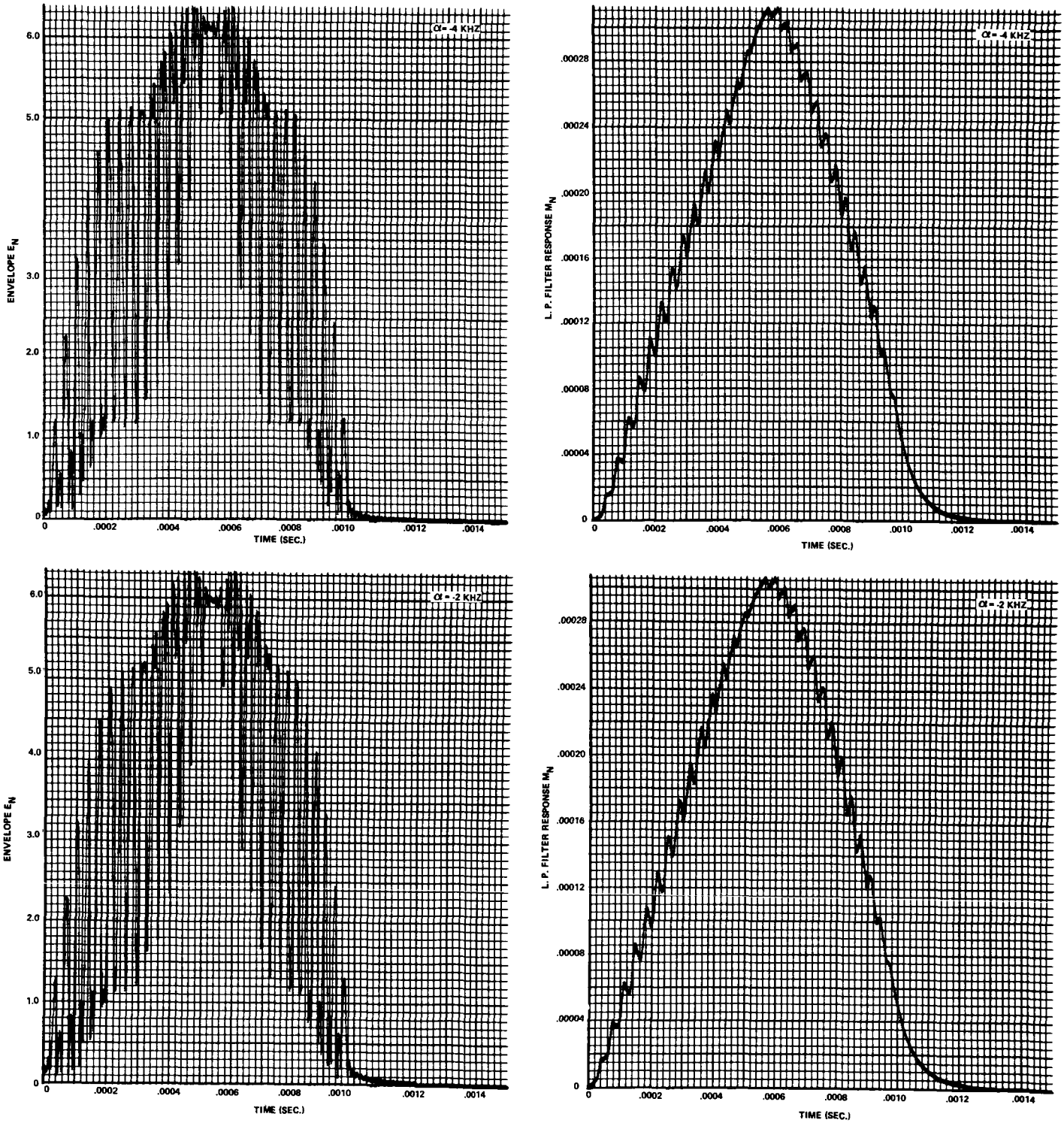

FIGURE 28 - GRAPHS OF E_N AND M_N FOR CASE II

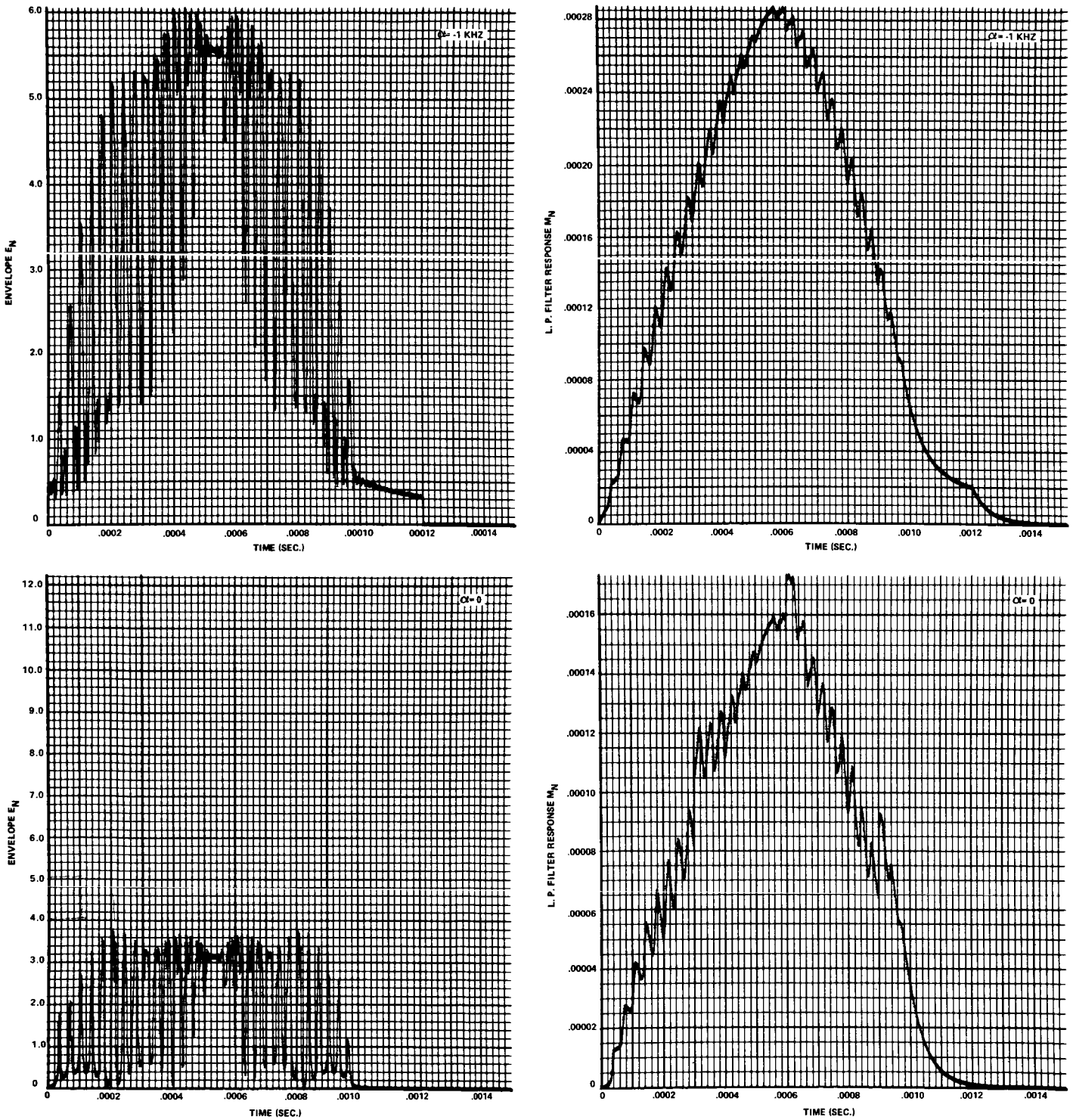

FIGURE 26 - GRAPHS OF E_N AND M_N FOR CASE II

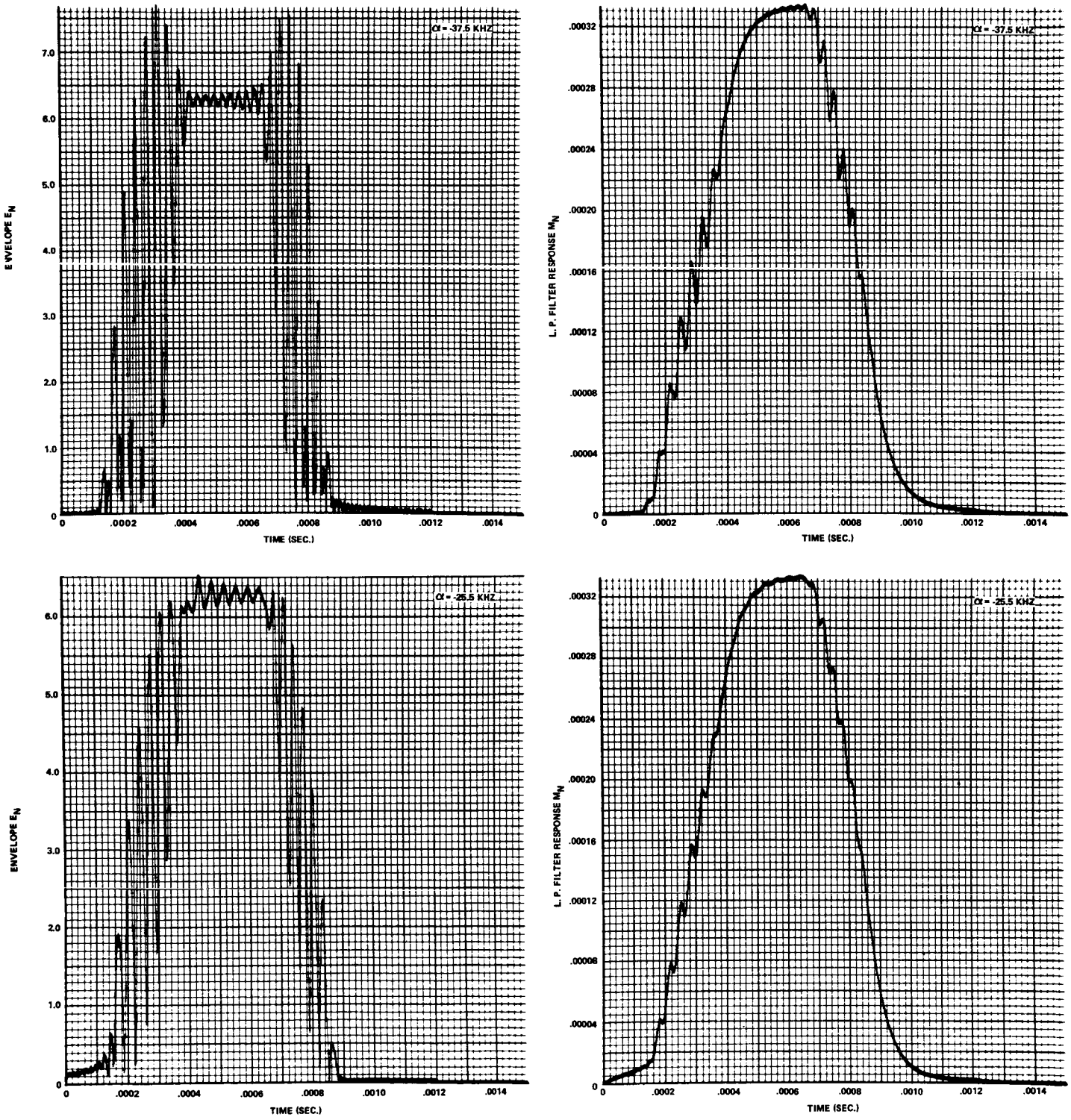

FIGURE 27 - GRAPHS OF E_N AND M_N FOR CASE III

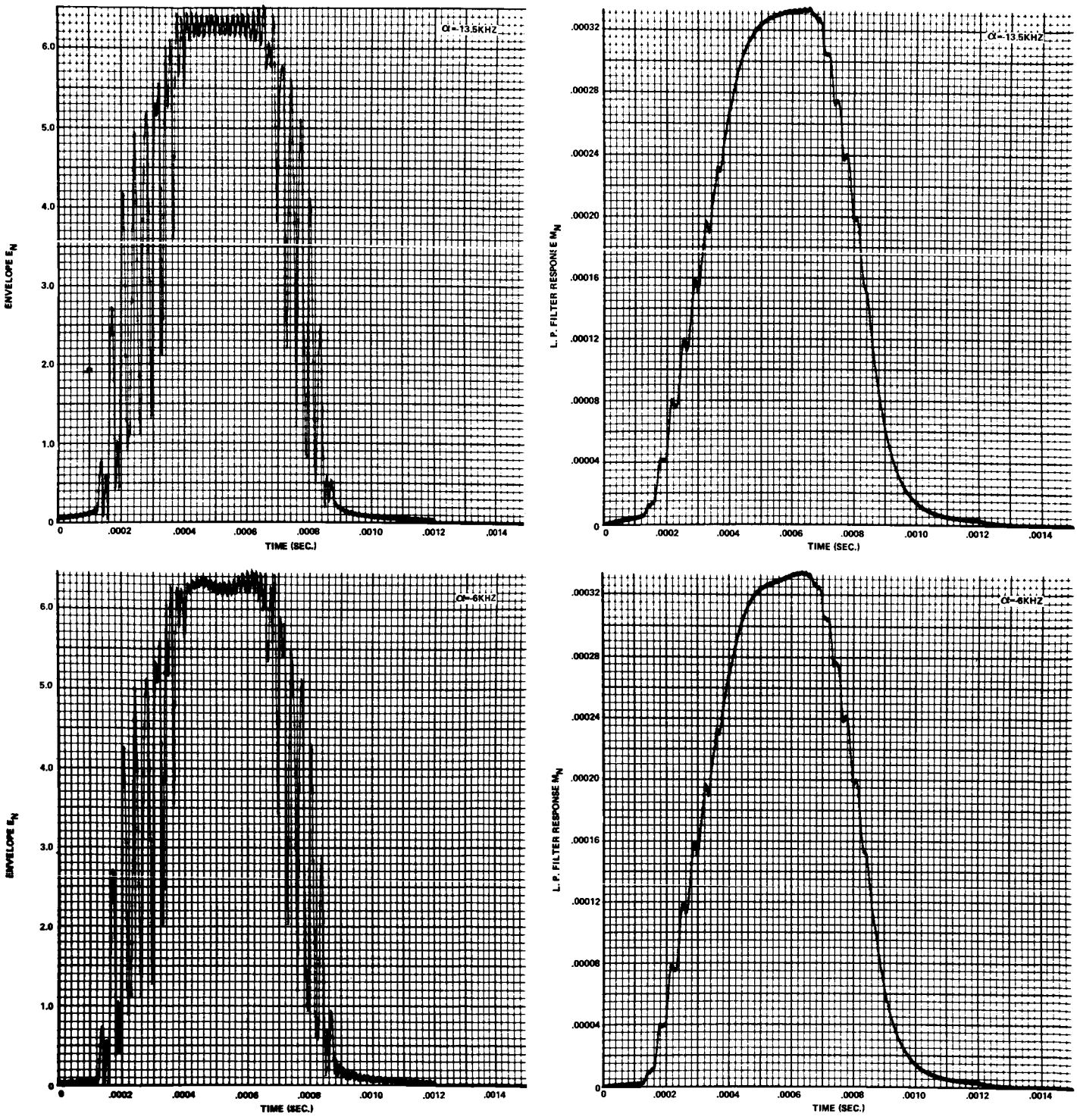

FIGURE 28 - GRAPHS OF E_N AND M_N FOR CASE III

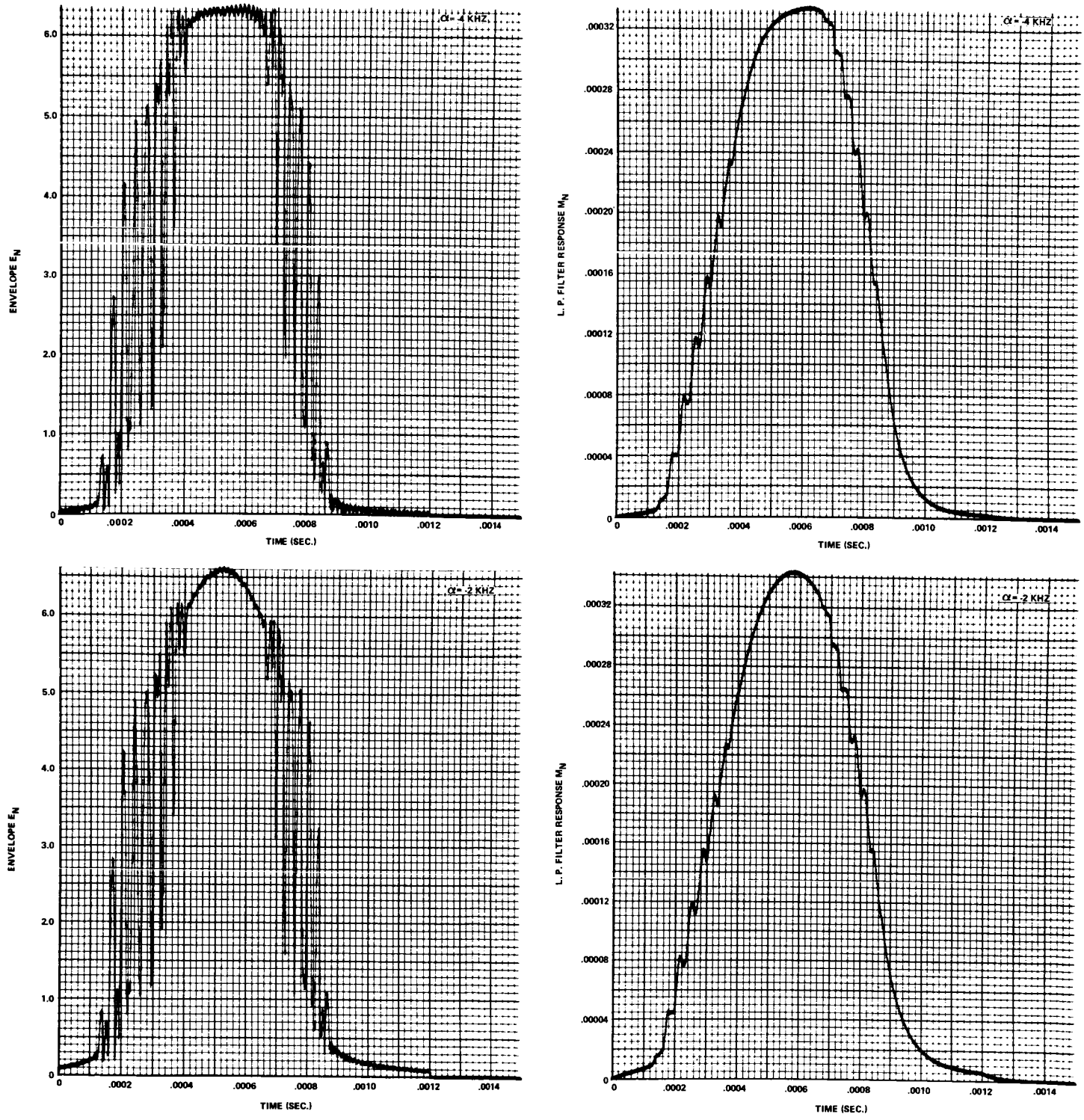

FIGURE 29 - GRAPHS OF E_N AND M_N FOR CASE III

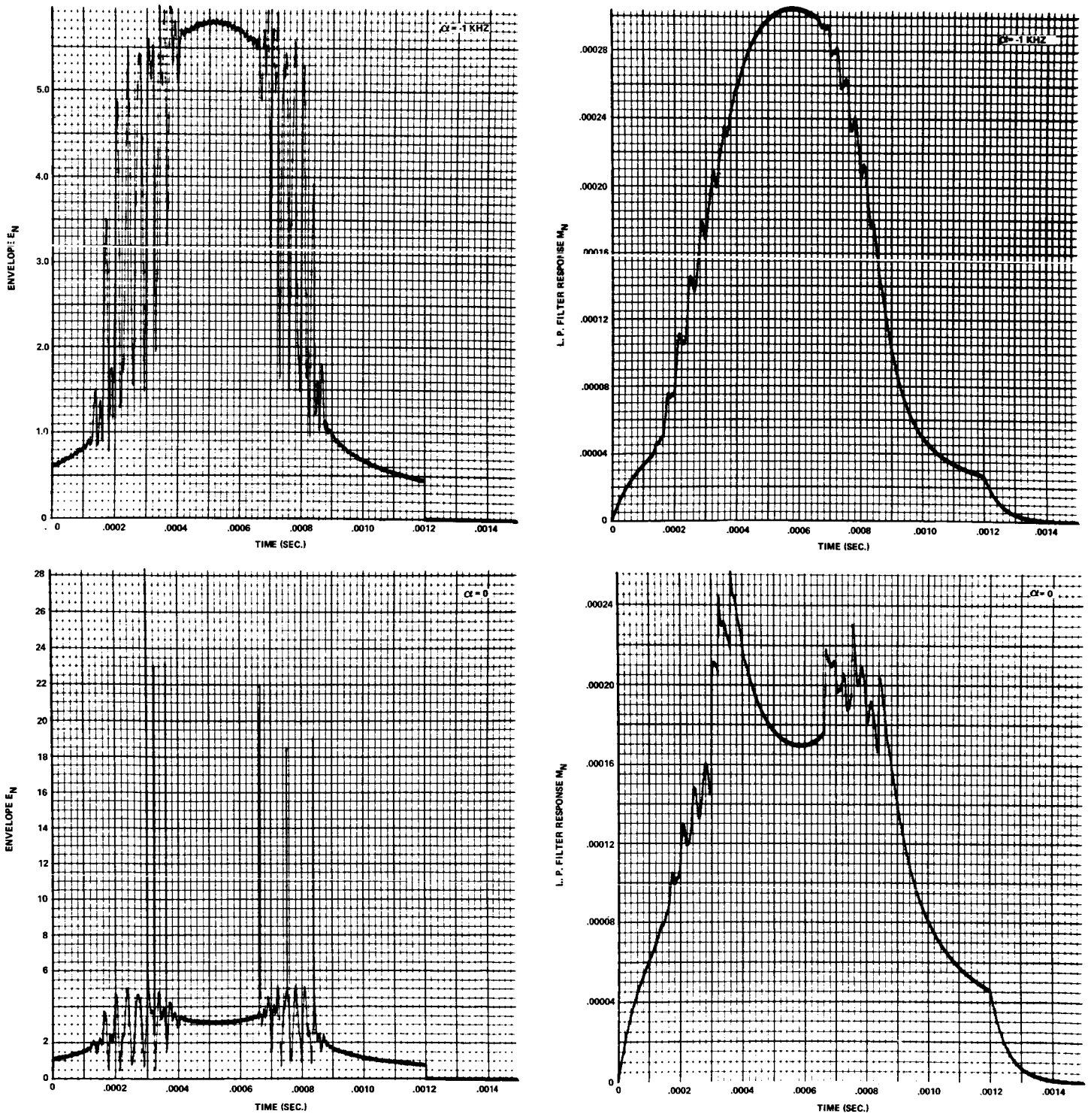

FIGURE 30 - GRAPHS OF E_N AND M_N FOR CASE III

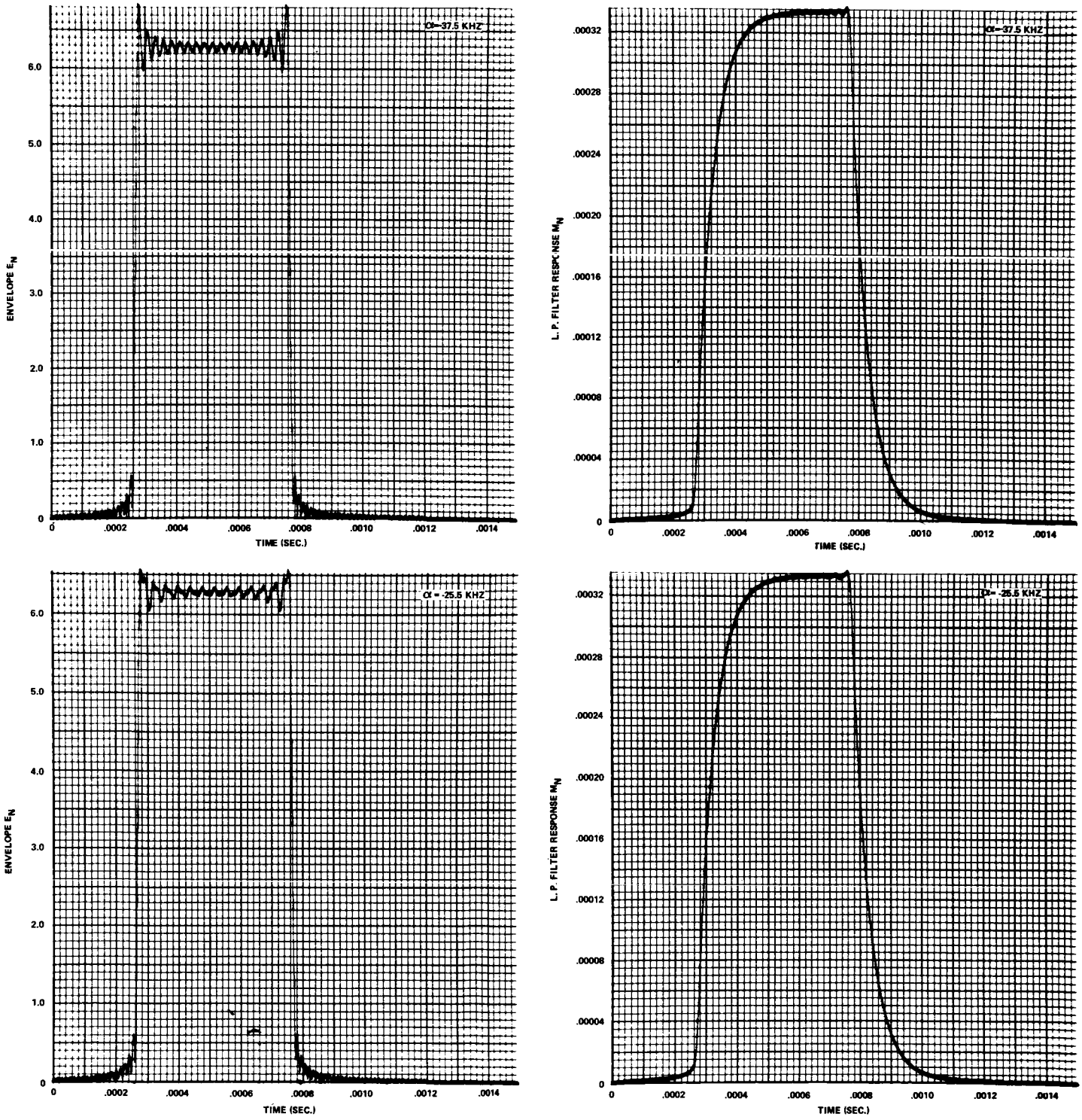

FIGURE 31 - GRAPHS OF E_N AND M_N FOR CASE IV

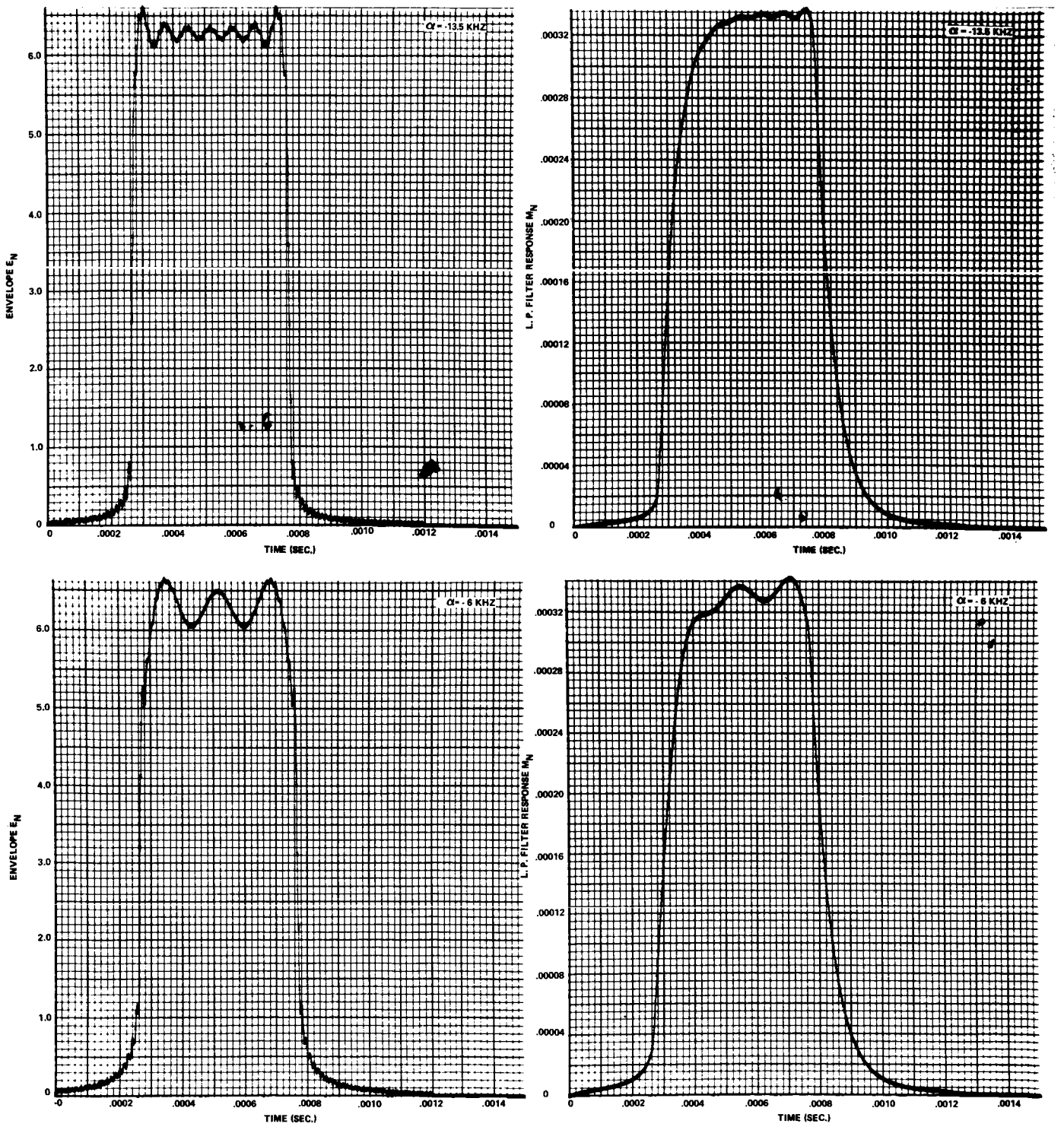

FIGURE 32 - GRAPHS OF E_N AND M_N FOR CASE IV

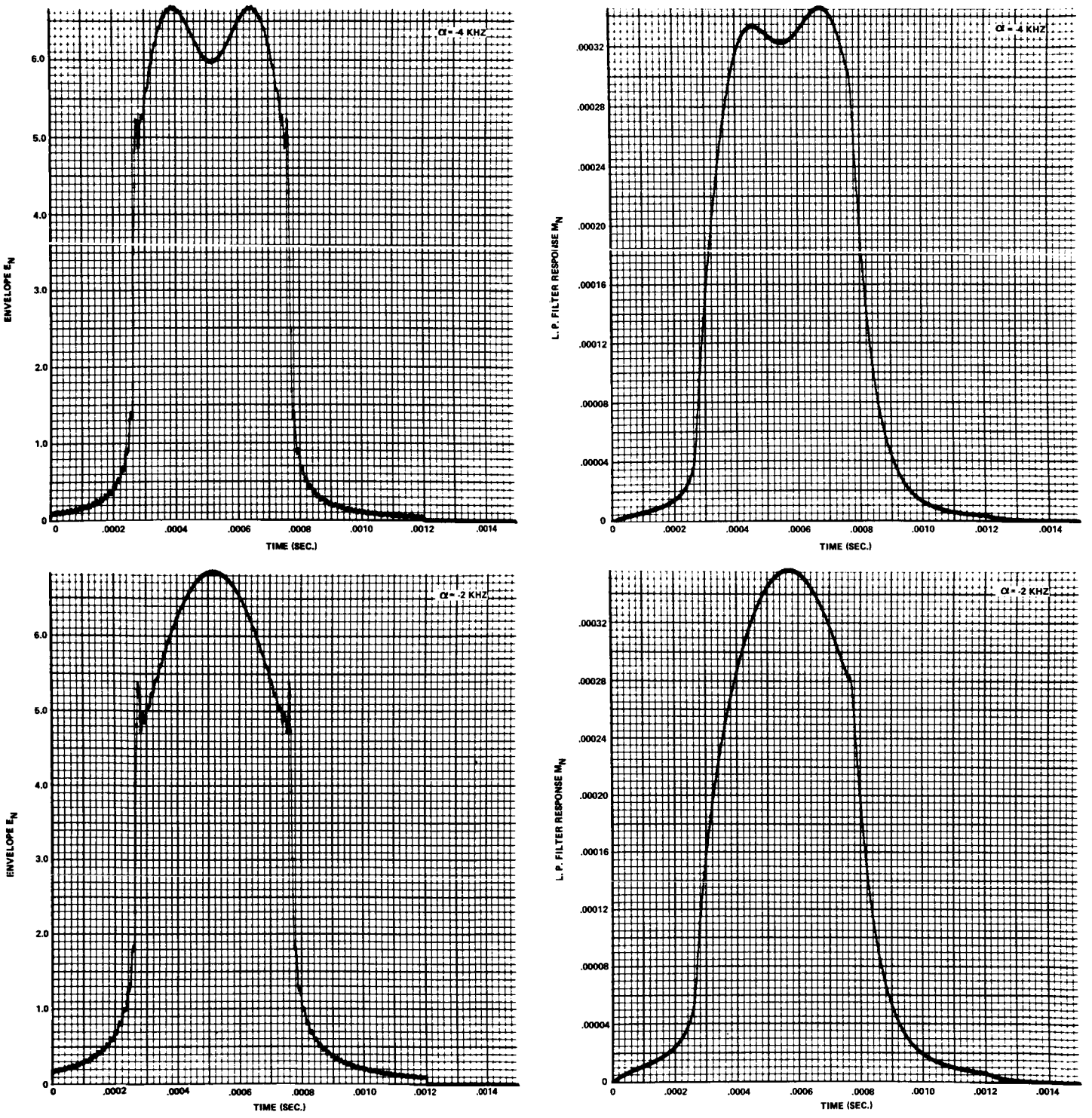

FIGURE 33 - GRAPHS OF E_N AND M_N FOR CASE IV

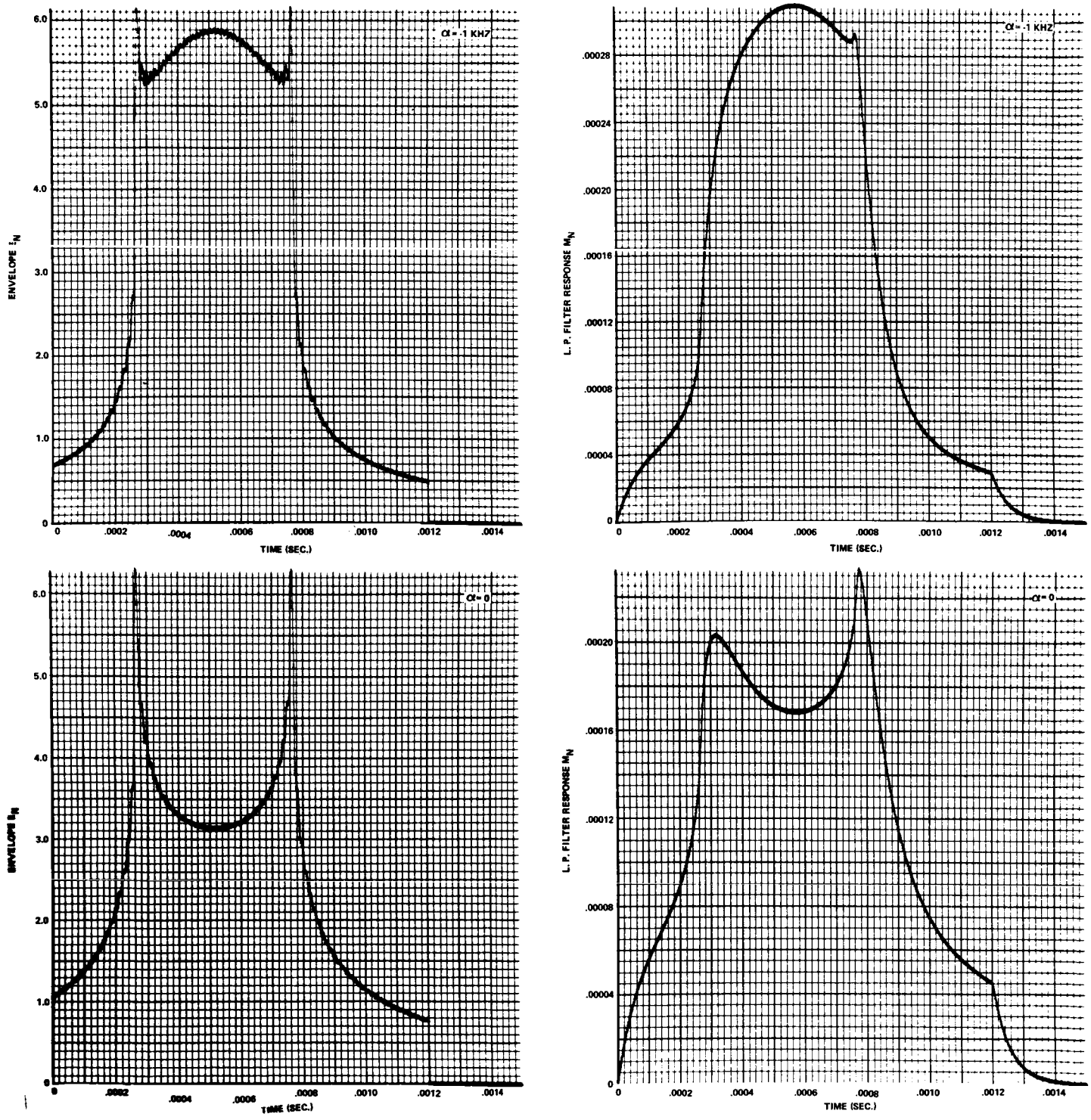

FIGURE 34 - GRAPHS OF E_N AND M_N FOR CASE IV

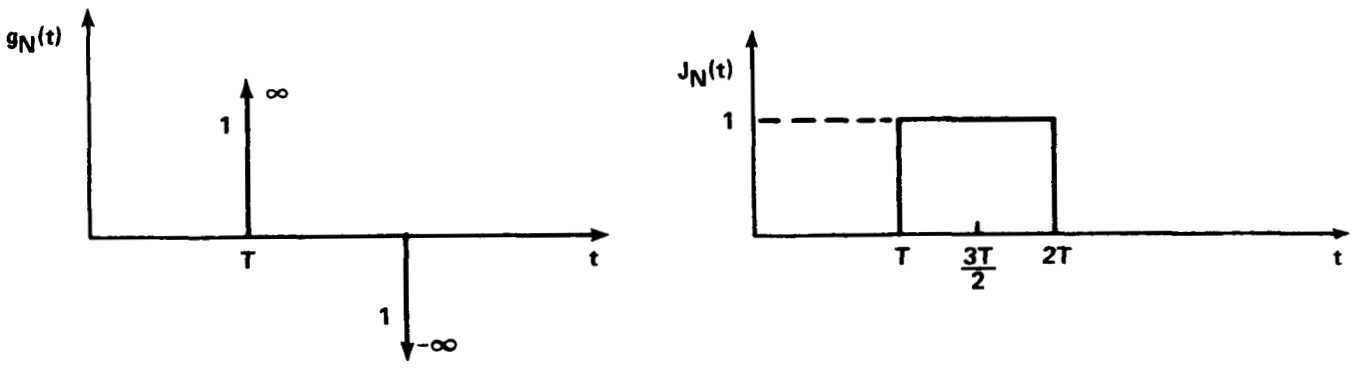

FIGURE 35 - GRAPHS OF g_N AND J_N FOR N = 1 AND f(1) = 1

APPENDIX I

RESPONSE OF A NARROW BANDPASS FILTER IN TERMS OF THE LOWPASS EQUIVALENT FILTER

The input to the AM receiver is

$$s = V\,J \cos \omega_c t \tag{1-1}$$

where $J = \int_{-\infty}^{t} g(x)dx$ is assumed to be narrowband limited around the origin on the frequency axis with respect to the frequency ω_c. That is, s is a narrowband signal. The response of the BP filter through which s passes is defined by r. In order to derive the response of the AM receiver the function r must be known. The expression for r in terms of s and an asymmetrical BP filter is derived in this Appendix.

Consider a BP filter that may be unsymmetrical about ω_c with the transfer function $H(j\omega)$. From $H(j\omega)$ two transfer functions are derived, $H_1(j\omega) = H(j\omega)\underline{u}_1(\omega)$ and $H_2(j\omega) = H(j\omega)\underline{u}_1(-\omega)$. These are related by $H(j\omega) = H_1(j\omega) + H_2(j\omega)$. Since $H(j\omega)$ is narrowband around ω_c, two lowpass transfer functions can be found by shifting H_1 and H_2 by ω_c. These are $H_{\ell_1} = H_1(\omega+\omega_c)$ and $H_{\ell_2} = H_2(\omega-\omega_c)$. Taking the sum and difference of H_{ℓ_1} and H_{ℓ_2}, two lowpass filters are defined by:

$$H_p(j\omega) = \frac{H_{\ell_1}(j\omega) + H_{\ell_2}(j\omega)}{2} \tag{1-2}$$

and

$$H_q(j\omega) = \frac{H_{\ell_2}(j\omega) - H_{\ell_1}(j\omega)}{2j}$$

APPENDIX I

These filters have the properties

$$H_p(-j\omega) = H_p^*(j\omega)$$

and

$$H_q(-j\omega) = H_q^*(j\omega)$$

Then if

$$h_p = F^{-1}[H_p(j\omega)] \tag{1-3}$$

and

$$h_q = F^{-1}[H_q(j\omega)]$$

these time functions are real and vary slowly with respect to $\cos\omega_c t$.

The impulse response of the BP filter $H(j\omega)$ is the real time function h related to h_p and h_q by

$$h = 2\, h_p \cos\omega_c t + 2\, h_q \sin\omega_c t \tag{1-4}$$

The response of the BP filter to the input s is r = s*h where (*) denotes convolution. The response to s is

$$\begin{aligned} r &= 2\int_{-\infty}^{+\infty} h_p(t-\tau)\cos(\omega_c t-\omega_c\tau)VJ(\tau)\cos\omega_c\tau d\tau \\ &+ 2\int_{-\infty}^{+\infty} h_q(t-\tau)\sin(\omega_c t-\omega_c\tau)VJ(\tau)\cos\omega_c\tau d\tau \\ &\cong V\int_{-\infty}^{+\infty} h_p(t-\tau)J(\tau)d\tau \cdot \cos\omega_c t \\ &+ V\int_{-\infty}^{+\infty} h_q(t-\tau)J(\tau)d\tau \cdot \sin\omega_c t \end{aligned} \tag{1-5}$$

APPENDIX I

The approximation is obtained by discarding two integrals in the r expression that have integrands with the factors $\cos(\omega_c t - 2\omega_c \tau)$ and $\sin(\omega_c t - 2\omega_c \tau)$. These integrals are approximately zero if h_p, h_q and J are lowpass and narrowband limited with respect to ω_c. Since

$$R_e\left[e^{j\omega_c t}(h_p - j\, h_q)\right] = h_p \cdot \cos\omega_c t + h_q \cdot \sin\omega_c t \qquad (1\text{-}6)$$

(1-5) becomes

$$r = V\, R_e\left\{e^{j\omega_c t}\int_{-\infty}^{+\infty}[h_p(t-\tau) - j\, h_q(t-\tau)] \cdot J(\tau)d\tau\right\} \qquad (1\text{-}7)$$

From (1-2), $H_{\ell_1}(j\omega)$ is the Fourier Transform of $h_p - j\, h_q$. Then (1-7) is

$$r = V\, R_e\left\{e^{j\omega_c t}\, F^{-1}[H_{\ell_1}(j\omega) \cdot F(J)]\right\} \qquad (1\text{-}8)$$

The response of H_{ℓ_1} to J is easier to obtain than the response of $H(j\omega)$ to s. Hence (1-8) is a very useful result for a narrow BP filter excited by a signal that is narrowband limited in the passband of the filter.

APPENDIX II

THE BANDPASS FILTER RESPONSE WHEN S IS A PDM-AM WAVEFORM

The signal s is a PDM-AM waveform if g in the s equation (1-1) is the impulse sequence

$$g(t) = \sum_{n=-\infty}^{+\infty} \left\{ \delta[t-nT] - \delta[t-(n+f(n)T)] \right\} \qquad (2\text{-}1)$$

The function $\int_{-\infty}^{t} g(x)dx$ is a non-overlapping sequence of square waves if $f(x)$ is limited to $0 \leq f(x) \leq 1$. This restriction will be placed on all functions $f(x)$ considered. When n is limited to the finite set of integers $n \varepsilon \{1,2,\ldots,N\}$, s in (1-1) becomes a PDM-AM waveform with finite duration. For the finite set of n, the integral J in (1-1) is

$$J_N = \sum_{n=1}^{N} \left[\underline{u}_1(t-nT) - \underline{u}_1[t-(n+f(n))T] \right] \qquad (2\text{-}2)$$

where $\underline{u}_1(t)$ is the unit step function at t=0. The response m_N of the AM receiver is of interest when the bandpass filter is narrowband around ω_c and the receiver input is $s_N = V\ J_N \cos\omega_c t$. To find m_N the intermediate function r_N at the BP filter output must be found. This response can be derived in terms of the low-pass equivalent of the BP filter and the lowpass function J_N. From (1-8)

$$r_N = V\ R_e \left\{ e^{j\omega_c t} \cdot F^{-1}[H_{\ell_1}(j\omega) \cdot F(J_N)] \right\} = \qquad (2\text{-}3)$$

$$V \sum_{n=1}^{N} Tf(n)\ R_e \left\{ e^{j\omega_c t} \cdot F^{-1} \left[H_{\ell_1}(j\omega)\ \frac{\sin(\omega Tf(n)/2)}{\omega Tf(n)/2} \cdot e^{j\omega[n+f(n)/2]T} \right] \right\}$$

At this point some form must be assumed for the BP filter characteristic $H(j\omega)$ if numerical results are desired from (2-3). Suppose the filter is described by the ideal characteristic:

$$H(j\omega) = \begin{cases} k & , \omega_c + \alpha \leq |\omega| \leq \omega_c + \beta \quad , \quad \alpha < \beta \\ 0 & , \text{all other } \omega \end{cases} \tag{2-4}$$

This filter is unsymmetrical around ω_c and is narrowband if $(\beta-\alpha) << \omega_c$. As defined in Appendix I,

$$H_{\ell_1}(j\omega) = H_1(j\omega+j\omega_c) = H(j\omega+j\omega_c)\underline{u}_1(\omega+\omega_c) .$$

Then from (2-4)

$$H_{\ell_1}(j\omega) = \begin{cases} k & , \alpha < \omega < \beta \\ 0 & , \text{all other } \omega \end{cases} \tag{2-5}$$

To find (2-3) the inverse transform of $H_{\ell_1} \frac{\sin \omega a/2}{\omega a/2}$ is found. This is

$$F^{-1}\left[H_{\ell_1} \cdot \frac{\sin \omega a/2}{\omega a/2}\right] =$$

$$\frac{k}{2\pi}\int_\alpha^\beta \frac{\sin \omega a/2}{\omega a/2} \cos\omega t \, d\omega +$$

$$j\,\frac{k}{2\pi}\int_\alpha^\beta \frac{\sin \omega a/2}{\omega a/2} \sin\omega t \, d\omega$$

$$= \frac{k}{2\pi}\,\frac{1}{a}\left\{\int_{\alpha(\frac{a}{2}+t)}^{\beta(\frac{a}{2}+t)} \frac{\sin y}{y}\,dy + \int_{\alpha(\frac{a}{2}-t)}^{\beta(\frac{a}{2}-t)} \frac{\sin y}{y}\,dy \right.$$

$$\left. + j\int_{\alpha(\frac{a}{2}-t)}^{\beta(\frac{a}{2}-t)} \frac{\cos y}{y}\,dy - j\int_{\alpha(\frac{a}{2}+t)}^{\beta(\frac{a}{2}+t)} \frac{\cos y}{y}\,dy\right\} \tag{2-6}$$

But

$$\int_{\alpha(\frac{a}{2} \pm t)}^{\beta(\frac{a}{2} \pm t)} \frac{\sin y}{y}\, dy = S_i[\beta(\tfrac{a}{2} \pm t)] - S_i[\alpha(\tfrac{a}{2} \pm t)] \qquad (2\text{-}7)$$

and

$$\int_{\alpha(\frac{a}{2} \pm t)}^{\beta(\frac{a}{2} \pm t)} \frac{\cos y}{y}\, dy = C_i[|\beta(\tfrac{a}{2} \pm t)|] - C_i[|\alpha(\tfrac{a}{2} \pm t)|] \qquad (2\text{-}8)$$

where

$$S_i(z) = \int_0^z \frac{\sin y}{y}\, dy$$

and

$$C_i(|z|) = -\int_{|z|}^{\infty} \frac{\cos y}{y}\, dy = -\int_z^{\infty} \frac{\cos y}{y}\, dy \quad . \qquad (2\text{-}9)$$

The integrals S_i and C_i are well known tabulated functions of z. The inverse of $H_{\ell_1} \frac{\sin \omega a/2}{\omega a/2}$ is found in terms of S_i and C_i functions by substituting (2-7) and (2-8) into (2-6). The only difference between $F^{-1}\left[H_{\ell_1} \cdot \frac{\sin \omega a/2}{\omega a/2}\right]$ and $F^{-1}\left[H_{\ell_1} \cdot \frac{\sin \omega a/2}{\omega a/2} \cdot e^{-j\omega x}\right]$ is a time shift of x seconds. Then the response of $H_{\ell_1}(j\omega)$ to the sequence J_N in (2-3) follows by inspection from (2-6). Introducing (2-6) into (2-3),

$$r_N = \frac{kV}{2\pi} R_e \left\{ e^{j\omega_c t} \sum_{n=1}^{N} [X_n + j\, Y_n] \right\}$$

$$= \frac{kV}{2\pi} \left[\cos\omega_c t \sum_{n=1}^{N} X_n - \sin\omega_c t \sum_{n=1}^{N} Y_n \right]$$

$$= \frac{kV}{2\pi} \left[\left(\sum_{n=1}^{N} X_n \right)^2 + \left(\sum_{n=1}^{N} Y_n \right)^2 \right]^{1/2} \cos[\omega_c t + \Psi]$$

$$= \frac{kV}{2\pi} e \quad \cos[\omega_c t + \Psi] \tag{2-10}$$

where

$$X_n = S_i[\beta(t - nT)]$$

$$- S_i[\alpha(t - nT)]$$

$$+ S_i[\beta(f(n)T - t + nT)]$$

$$- S_i[\alpha(f(n)T - t + nT)]$$

and

$$Y_n = - C_i[|\alpha(f(n)\ T - t + nT)|]$$

$$+ C_i[|\beta(f(n)\ T - t + nT)|]$$

$$+ C_i[|\alpha(t - nT)|]$$

$$- C_i[|\beta(t - nT)|]$$

The phase of r_N is $\Psi = \tan^{-1}\left(\sum Y_n / \sum X_n\right)$.

The envelope of r_N is $\frac{kV}{2\pi} e = E_N$. It is this function that the envelope detector produces for lowpass filtering in the AM receiver. For the case of symmetrical bandpass filtering where $\alpha = -\beta$, all Y_n terms are zero and $e = \sum X_n$. If, in addition, $f(n) = 1$ for $n = 1,2...,N$; than $e = 2\ S_i[\beta(t-T)] - 2\ S_i[\beta(t-[N+1]T)]$. This is the well known square wave response of an ideal symmetrical lowpass filter of bandwidth 2β where the input pulse width is NT.

APPENDIX III

THE AVERAGE POWER SPECTRUM OF $S_N(t)$

The power spectrum of S is easily found if n in (2-1) is limited to the finite set $n\varepsilon\{1,\ldots,N\}$. Then s becomes $s_N = V\ J_N \cos\omega_c t$ where J_N is the integral of the finite sequence of impulses

$$g_N = \sum_{n=1}^{N} \{\delta[t - nT] - \delta[t - (n + f(n))T]\} \tag{3-1}$$

The transform of (3-1) is

$$G_N(j\omega) = \sum_{n=1}^{N} \{\exp[-j\omega nT] - \exp[-j\omega(n + f(n))T]\} \tag{3-2}$$

where

$$\int_{-\infty}^{\infty} \delta[t - T(n + f(n))] \exp[-j\omega t]\, dt = \exp[-j\omega T(n + f(n))] \tag{3-3}$$

has been used. The power spectrum of the finite duration g_N $|G_N|^2 = G_N \cdot G_N^*$. Then

$$|G_N|^2 = \sum_{n=1}^{N} \sum_{m=1}^{N} \{\exp[-j\omega T(n-m)] - \exp[-j\omega T[(n + f(n)) - m]] - \exp[-j\omega T[n-(m + f(m))]] + \exp[-j\omega T[(n + f(n)) - (m + f(m))]]\} \tag{3-4}$$

For the first exponential in (3-4)

$$\sum\sum \frac{1}{2} \exp[j\omega T(m-n)] = \sum\sum \frac{1}{2} \exp[j\omega T(n-m)] \tag{3-5}$$

Then

$$\sum\sum \exp[-j\omega T(n-m)] = \sum\sum \cos(n-m)\omega T \tag{3-6}$$

Likewise it is found that,

$$\begin{aligned} &\sum\sum \exp[-j\omega T[(n + f(n)) - (m + f(m))]] = \\ &\sum\sum \cos[(n + f(n)) - (m + f(m))]\omega T \end{aligned} \tag{3-7}$$

Also in (3-4),

$$\begin{aligned} &\sum\sum \{\exp[j\omega T[m - (n + f(n))]] + \exp[-j\omega T[n - (m + f(m)]]\} \\ &= 2\sum\sum \cos[n - (m + f(m))]\omega T \end{aligned} \tag{3-8}$$

Combining the last three equations in (3-4) gives

$$\begin{aligned} |G_N|^2 = \sum_{n=1}^{N} \sum_{m=1}^{N} \{&\cos[n-m]\omega T + \\ &\cos[n + f(n) - m - f(m)]\omega T \\ &- 2 \cos[n - m - f(m)]\omega T\} \end{aligned} \tag{3-9}$$

Since the AM in s is the integral of g, the power spectrum of the AM for the finite case $g = g_N$ is $|G_N|^2/\omega^2$. This follows from the transform of $\int_{-\infty}^{t} g_N \, dx$ which

is $(j\omega)^{-1} F[g_N]$. With $J_N = \int_{-\infty}^{t} g_N(x)dx$ and $T_N(j\omega) = F[J_N]$, the AM power spectrum is

$$|T_N|^2 = \sum_{n=1}^{N} \sum_{m=1}^{N} \frac{1}{\omega^2} \{\cos[n-m]\omega T - 2\cos[n - m - f(m)]\omega T + \cos[n + f(n) - m - f(m)]\omega T\} \tag{3-10}$$

The power spectrum of s is simply

$$S_s(\omega) = \frac{1}{2}\left[|T_N|^2_{\omega\to\omega+\omega_c} + |T_N|^2_{\omega\to\omega-\omega_c} \right] . \tag{3-11}$$

As an example of the result (3-10), let N = 1 and f(1) = 1. Then g_N and J_N are shown in Figure 35.

With N = 1, f(1) = 1,

$$T_N(j\omega) = \exp[-j\ 3\omega T/2] \cdot T \frac{\sin \omega T/2}{\omega T/2}$$

and

$$|T_N|^2 = \left[\frac{T \sin \omega T/2}{\omega T/2}\right]^2$$

For this simple example,

$$S_s(\omega) = \frac{1}{2}\left[\frac{T \sin(\omega+\omega_c)T/2}{(\omega+\omega_c)T/2}\right]^2 + \frac{1}{2}\left[\frac{T \sin(\omega-\omega_c)T/2}{(\omega-\omega_c)T/2}\right]^2$$

The spectrum of s_N follows from (3-10) and (3-11) when N and f(x) are given. Since the summations involved are usually difficult, a computer program was written to find $|T_N|^2$.

TM 70-2034-5

TECHNICAL MEMORANDUM

PATH LOSS EXPRESSIONS FOR A RADIO LINK ON A ROUGH SPHERICAL SURFACE

Bellcomm

ACCESSION NUMBER
PAGES
NASA CR OR TMX OR AD NUMBER
AVAILABLE TO U.S. GOVERNMENT AGENCIES ONLY